CHALMERS
UNIVERSITY OF TECHNOLOGY

Design and analysis of wireless charging combined with conductive charging

Master's thesis in Electric Power Engineering

VIKTOR BERNTSSON

Department of Energy and Environment
CHALMERS UNIVERSITY OF TECHNOLOGY
Gothenburg, Sweden 2017

Master's thesis 2017

Design and analysis of wireless charging combined with conductive charging

Viktor Berntsson

Department of Energy and Environment
Division of Electric Power Engineering
Chalmers University of Technology
Gothenburg, Sweden 2017

Design and analysis of wireless charging combined with conductive charging
VIKTOR BERNTSSON

Supervisor: Daniel Pehrman, Department of Energy and Environment
Examiner: Yujing Liu, Department of Energy and Environment

Master's Thesis 2017
Department of Energy and Environment
Division of Electric Power Engineering
Chalmers University of Technology
SE-412 96 Gothenburg
Telephone +46 31 772 1000

Typeset in LaTeX
Printed by Chalmers Reproservice
Gothenburg, Sweden 2017

Design and analysis of wireless charging combined with conductive charging
VIKTOR BERNTSSON
Department of Energy and Environment
Chalmers University of Technology

Abstract

One way to reduce the amount of emissions from vehicles is to replace the combustion cars with electrical vehicles. To encourage people to do this the electrical vehicles needs to be improved but also the way of charging them. It is necessary that the way of charging an electrical vehicle is both more efficient and convenient than filling the gas tank of a combustion car. This is one argument to convince people that electrical vehicles are an adequate alternative instead of the combustion cars. Inductive charging will make the charging procedure easier due to that the driver only needs to park over the charging plate and then leave the car. This is an easier way of charging an electrical vehicle due to that the driver does not have to do anything except park the car compared to conductive charging where the driver needs to plug in the cable every time the vehicle needs to be charged. In this thesis, a new concept of charging will be brought up where the driver can choose between charging wirelessly or through a cable with the same system. This is done by designing and simulating one inductive and three conductive systems separately. These systems will then be combined into one system which can handle both inductive and conductive charging. The systems are designed for 3.3 kW and the simulations shows an efficiency between 85.98 $-$ 92.53% for the inductive system and an efficiency between 92.84 $-$ 98.42% for the conductive systems. The inductive system will have a high leakage inductance, therefore capacitor banks are placed in series with the coils for the inductive system to increase the amount of transferred power between the coils. The inductive system is calculated to cost 4695 SEK and the conductive systems is calculated to cost between 3485 $-$ 3820 SEK. By combining these two system it is predicted that the combined system is going to be able to handle both inductive and conductive charging to the cost of approximate 73 % of two separate systems without affecting the performance.

Keywords: Inductive power transfer, Inductive charging, conductive charging, electric vehicle charger.

Acknowledgements

I would like to thank my supervisor Daniel Pehrman for his expertise, guidance and support during the project. I would also like to thank my examiner Prof. Yujing Liu for his helpful suggestions in this project.

Viktor Berntsson, Gothenburg, June, 2017

Contents

1 Introduction **1**
1.1 Background . . . 1
1.2 Aim . . . 3
1.3 Task . . . 3
1.3.1 Sustainable Development and Ethical Aspects . . . 4
1.4 Scope . . . 4
1.5 Structure . . . 4

2 Conductive charging of a EV **7**
2.1 Topologies/Components . . . 7
2.2 Induction and Transformer . . . 10
2.3 Standards and Application . . . 13

3 Inductive Charging **17**
3.1 Compensation . . . 18
3.2 Ferrite bars . . . 20

4 Methods (Power Electronic) **23**
4.1 Boost AC/DC converter in PFC application . . . 23
4.2 DC/DC Converter for Conductive Charging . . . 25
4.3 Setup for inductive charging . . . 33
4.4 Setup for combined system . . . 38

5 Results **41**
5.1 Simulation results for the Boost Converters . . . 41
5.2 Simulation results for the DC/DC steps . . . 46
5.3 Cost analysis . . . 63

6 Discussion **65**
6.1 Sustainable Development and Ethical Aspects . . . 67

7 Conclusion **71**

Bibliography **73**

1
Introduction

This chapter will introduce the reader to the background of the project.

1.1 Background

The number of registered passenger cars has increased almost every year during the last 70 years in Sweden [1]. Since 2006 the number of registered passenger cars has been higher than the number of deregistered passenger cars, except during 2013, which intends that the number of registered cars will keep increasing in the upcoming years [2]. Due to that most of the newly registered vehicles are driven by fossil fuels the amount of emissions and greenhouse gases from the vehicles will continue to pollute the environment. One way of reducing the amount of emissions and greenhouse gases is to replace the combustion car with a plug-in hybrid, PH, or an electrical vehicle, EV. These types of vehicles have been on the market for several years now and to be able to make these vehicles even more desirable, not only the performance needs to be improved but also the way of charging the vehicle needs to be improved.

The most common way of charging a PH, or an EV is by connecting a cable from the power outlet to the vehicle. This might be an obstacle for the customer due to several conditions, for example: greasy and/or dirty cable, stiff or clumsy cable, laziness or occupied hands by the user. These problems could be solved by using wireless charging instead which means that the only thing that the driver needs to do is to park the vehicle over a charging plate. It also provides with a safer system due to that the user does not need to touch the system. This means that the risk of getting an electrical chock from the cable is reduced. Wireless charging may be more convenient to use than standardised cable charging but it also brings some problems like leakage fields and high costs. The problem with leakage fields is that it may damage the nerve system if the human body is exposed to high magnetic fields. The Swedish Radiation Safety Authority has provided so called reference values for different places and devices which are recommendations. These are set to a fiftieth of the value where negative health effects can be observed. The reference value differs for different frequencies, this is due to that currents are more likely to be induced inside the human body for different frequencies. For example, for 50 Hz the reference value is 100 T [3]. A need of accurate positioning of the vehicle so misalignment does not appear is also important. The distance between the transmitter and receiver might be a problem if it becomes too far. The coils will be mainly surrounded by air which will make the magnetic field weak which will decrease the transferred power compared to a cable setup. The efficiency for wireless charging is for some cases almost as high as for cable charging.

The setup that is used for wireless and cable charging can be seen in Figure 1.1 and 1.2, respectively. As can be seen both system contains the same components. This does not mean that, for example, the rectifier or the frequency converter looks exactly the same but they both appear in the setup for wireless and conductive charging. However, one thing that separates these two setups is that wireless charging uses an air core and cable charging uses an iron core in the transformer. The setups will be more deeply discussed in theory chapters about conductive charging and inductive charging.

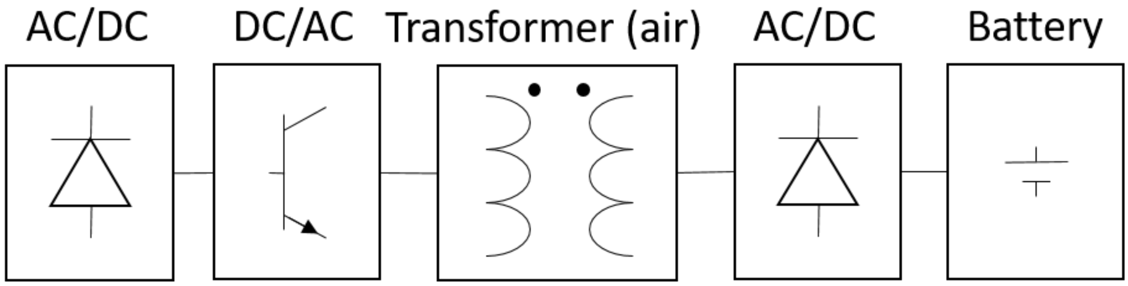

Figure 1.1: Setup for wireless charging.

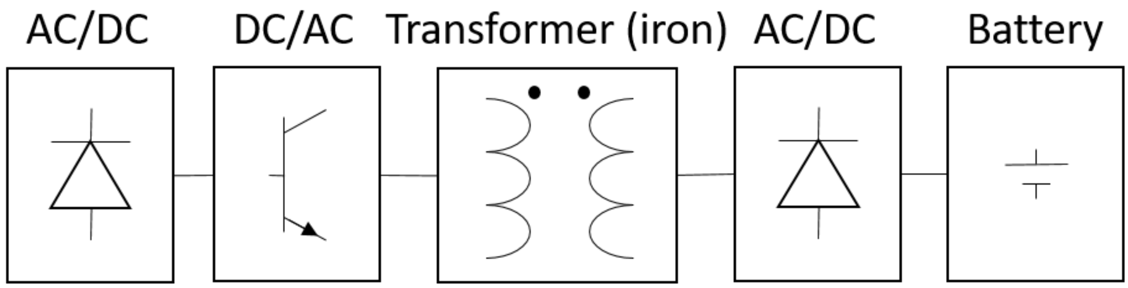

Figure 1.2: Setup for cable charging.

Both systems have their own advantages and disadvantages and due to that the two systems have four out of five equal components a combination of these two systems provide with an interesting new way of charging an electrical vehicle. The two systems can be used in either a series or a parallel setup. If it is connected in parallel all components from the two systems will be used. If it is connected in series it may be possible to reduce the number of components due to that the two systems will use the same components. Therefore, this report will focus mostly on the topology in series. The setup for these two systems combined can be seen in Figure 1.3. With this system, it is possible for the driver to choose between charging the EV wirelessly or with a cable. This solution also means that two types of vehicles can use the system, both vehicles that usually is charged by a cable and vehicles which will be charged wirelessly in the future. This means that for example, if a driver is looking for a parking spot with a wireless charging system and the only free spot has a cable system, the driver cannot charge the vehicle, or vice versa. This kind of problem needs to be solved to encourage more people to buy and drive an electrical vehicle instead of a regular vehicle with a combustion engine.

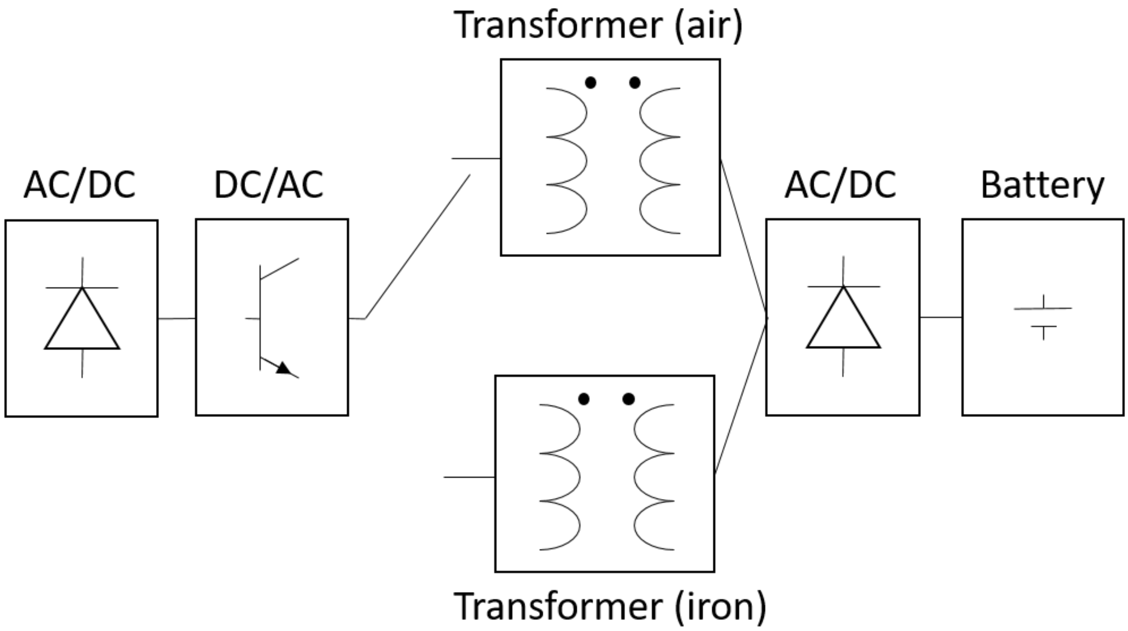

Figure 1.3: Setup for wireless and cable charging combined.

1.2 Aim

The aim of this project is to design and analyse a system, in a software, that combines the possibilities of charging a car battery wirelessly and through a cable.

1.3 Task

The aim can be divided into several tasks. First, these two charging systems are analysed separately and second these two system should be combined in the way as was showed in Figure 1.3 and be simulated. After that, the simulations will be analysed. The third task consist of a cost analysis for the new system and it will be investigated if this combined system is cheaper than a wireless system plus a cable system. If so, it may have the possibility and capability to someday hit the market. The forth task will consist of taking measurements, for the wireless case, on a similar system with already prebuilt components. The measurements will be compared with the simulated values.

1.3.1 Sustainable Development and Ethical Aspects

The problem with EVs today is that the performance compared to a combustion vehicle is not high enough. Usually it is the mileage that is too low for the EV and therefore a combustion vehicle is usually chosen instead of an EV. However, what will happen when the mileage of the EV is increased? Will the convenience of driving an EV increase and maybe even pass the convenience of driving a combustion car? The amount of EVs will probably increase but what will happen with the combustion cars? Will they be replaced or will only the amount of EVs increase and keep the amount of combustion cars unchanged? What will then happen with the greenhouse gases? Will it decrease if the combustion cars are replaced by EVs where the electricity is produced with coal and oil? These questions, together with questions that concern economical as well as a social aspects, will be discussed and answered. The natural question that will be related to the sustainable development is, "How is development of EV chargers actually making the world more sustainable?"

When it comes to the ethical aspects of doing a project like this it is important too make sure that both the positive and the negative sides of the results are presented to give the reader as accurate information as possible. This report is supposed to open up new doors and promote new and exciting ways of charging an EV. Therefore the first statement concerning ethics will be defined as "Show correct results from the simulations and the conclusions that are made should be backed up with correct data". The second ethical aspect follows up naturally as "Make a fair comparison between the conductive, inductive and the combined system". Also it is important that assumptions are based on facts and are not just random numbers. For the third and final aspect of the ethical discussion it is important to be aware of that humans and animals can get hurt if exposed to the magnetic field. Therefore the last question is defined as "How can damages from the magnetic field be avoided?".

1.4 Scope

The power level for the charging systems will be designed for 3.3 kW but the charging systems will be analysed from $1 - 7\ kW$. The systems will be designed for one phase and the switching frequency that will be used is 85 kHz. The resistance and inductance in the system will be either calculated or estimated, with respect to the properties of the materials for each component. During the measurements, only the prebuilt components will be available and no new components will be built. Misalignment and distance changes for the inductive charging system will be represented by increasing and decreasing the coupling factor of the transformer.

1.5 Structure

This first chapter is supposed to introduce the reader to why this project was made. The two following chapters will present some standards and information about conductive and inductive charging, respectively, and introduce how EVs are charged today. In the following chapter the reader will be provided with theory about how the different components for the different systems are designed. After that, the measurement and the simulation results will be presented and discussed. The project itself will then be discussed in the following chapter and in the final chapter the conclusions from this project will be stated.

2

Conductive charging of a EV

To be able to charge an EV a connection between the grid and the battery is required. This connection is referred to as a charger. In this chapter the reader will be provided with the necessary information that is needed to understand the concept of conductive charging.

Conductive charging can be done with several methods and with different power levels. The battery must be charged with DC but the charging station, which is connected to the grid, can supply either AC or DC. In the DC case, the current is rectified inside the charging station and in the AC case the current is rectified inside the EV, so called on board charger, OBC. When charging an EV it is possible to use either one phase or three phases. The number of phases depends on the desired power level which in turn will affect the charging time. High power means lower charging time and vice versa, but when using high power it is important to make sure that the equipment, such as cables and contacts, can withstand the high power. It is also important to make sure that the equipment can withstand different environments such as high and low temperatures, high and low humidity etc. This is due to that an EV should be able to be driven in any country in the world.

2.1 Topologies/Components

A charger consists of two parts, a rectifier with power factor correction, PFC, and a DC/DC converter. The rectifier is usually designed with a boost converter topology. The boost converter is equipped with a controller that consists of an output voltage controller with an inner current controller. It is added to make sure that the correct output voltage is achieved and it also controls that the power factor is as close to 1 as possible by controlling the input current. Note that the controller will not be designed in this project. The circuit of the rectifier with the boost topology can be seen in Figure 2.1.

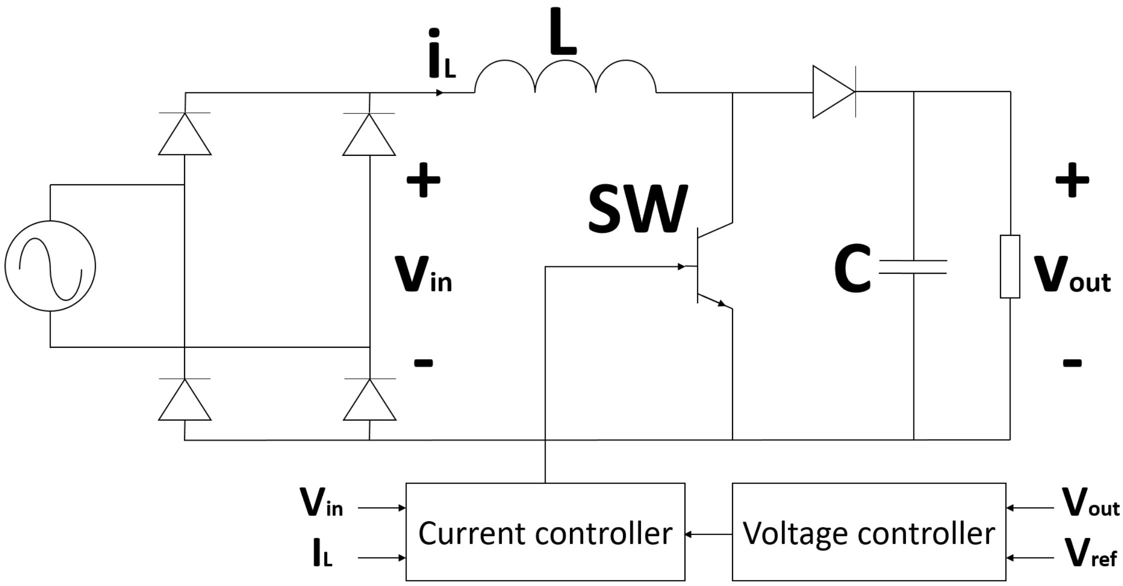

Figure 2.1: Rectifier with PFC and boost topology.

The goal of boost converter is to boost the output voltage, which means that the output voltage will be higher than the input voltage. This is done by charging the inductor while the switch is on and when the switch is turned off the power in the inductor is transferred to the load. A boost converter can be used in three different states, continuous conduction mode(CCM), discontinuous conduction mode (DCM) and boundary conduction mode(BCM). CCM means that the current through the inductor is always bigger than zero while during DCM the current through the inductor is zero during a short time during each switching period. BCM is achieved in the boundary between CCM and DCM.

By adding another boost converter in parallel, an interleaved boost converter can be achieved. The benefits of this topology is that it contains two energy sources with one switch each and the idea is that the ripple from the inductors should interfere and cancel each other. By cancelling the ripple, a smaller capacitance can be used on the output. The ripple is cancelled out due to that the two boost converters are phase shifted 180° to each other. When the duty cycle is reduced to half, the ripple can be reduced to half [4]. The circuit for the interleaved boost converter can be seen in Figure 2.2.

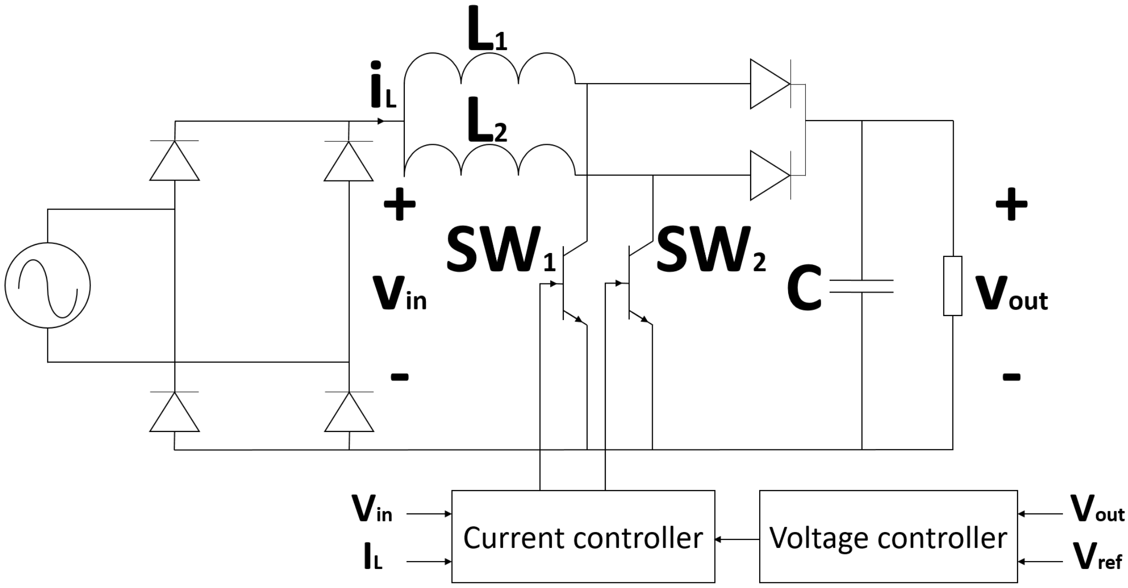

Figure 2.2: PFC with rectifier and a interleaved boost topology.

The DC/DC converter consists of an inverter, a transformer and a rectifier. When dealing with on board charging the DC/DC converter provides with galvanic isolation due to the transformer, it also controls the current to the battery. The circuit for the DC/DC converter can be seen in Figure 2.3. It can be seen that each switch is equipped with a diode and a capacitance in parallel, this is the anti-parallel diode, that all MOSFETs have, and the stray capacitance of the MOSFET. These are used to achieve zero voltage switching, ZVS, to lower the switching losses. The inverter usually is controlled with a phase shifted control which means that the switches is turned on and off in a specific way. The transformer does not only provide with electrical isolation, it also scales the voltage and the current. The power is then rectified and filtered before it reaches the battery. The design of the DC/DC converter and how to lower the losses will be more deeply discussed in chapter 4.

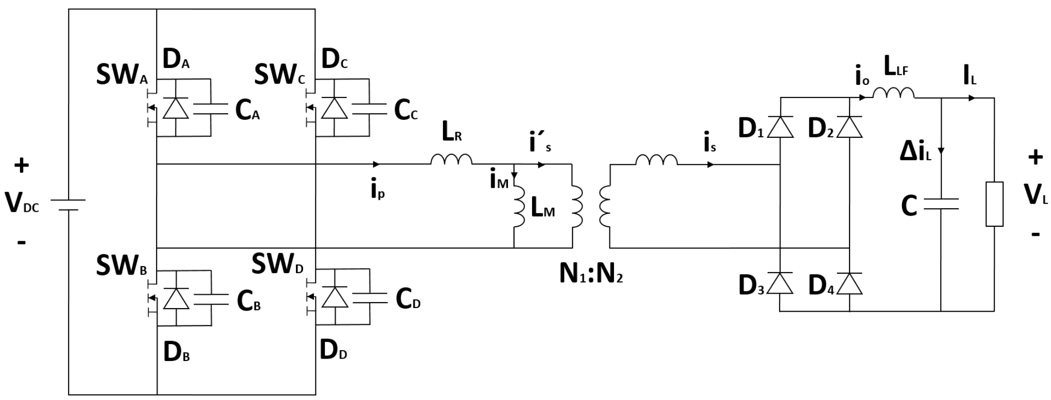

Figure 2.3: DC/DC converter with transformer as galvanic isolation.

It is also possible to use synchronous rectifiers which means that the diodes are replaced with MOSFETs. This makes the circuit more complex but it reduces the conduction losses. It is also possible to use just one leg and split the transformer on the secondary side. This means that fewer components will be used but each components has to withstand higher stresses.

When it come to fast charging of an EV the battery in the EV can be charged by a stationary storage battery which is connected to the grid. The storage battery is used to supply the battery in the EV with high currents which is necessary for fast charging. The reason for why the high currents can not be taken directly from the grid is due to that the grid is not designed to supply big loads during short and discontinuous time periods. Also plugs and connectors can not withstand such high currents. The circuit for this setup can be seen in Figure 2.4. The fast charging system is based on three phases and due to the high power level the system gets too big to be inside a car, so fast charging is refereed to as off board.

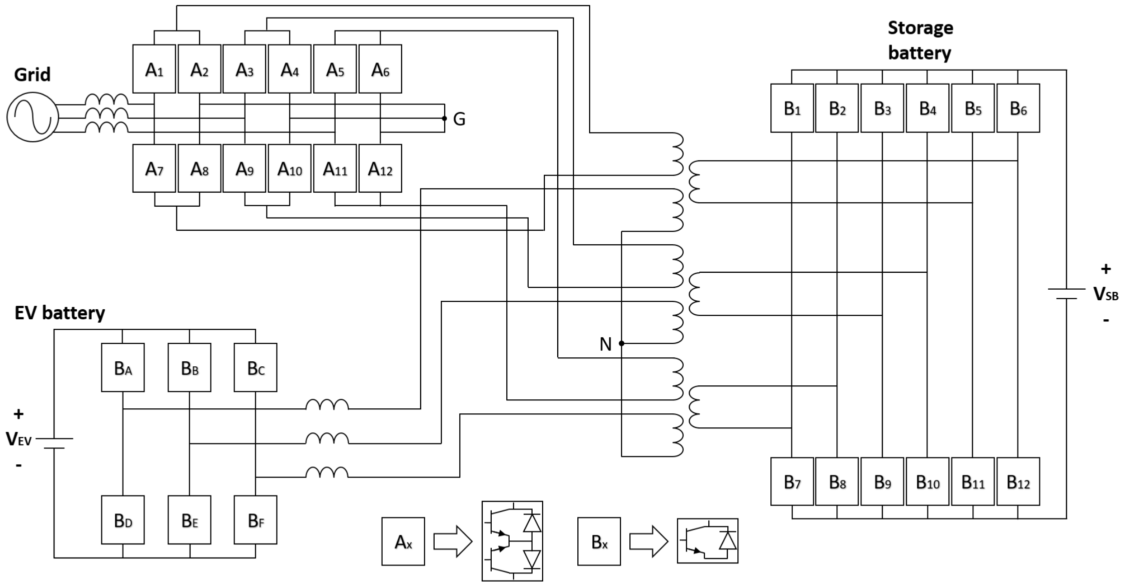

Figure 2.4: Setup for fast charging system.

2.2 Induction and Transformer

As mentioned before a transformer is used both for inductive and conductive charging. Therefore the concept of induction will be presented followed up by a description of a transformer. The theory is based from [5].

Faraday's law of induction describes the non-conservative electric field, E, when a variation in the magnetic flux density, B, appear, see (2.1)

$$\nabla \times E = -\frac{\partial B}{\partial t}. \tag{2.1}$$

By applying Stokes theorem, see (2.2) where F is a function, Faraday's law can be written in a form of an integration, see (2.3). This equation is valid for all geometries with an surface S and a contour C. The vector dA is an infinitesimal vector element of surface S.

$$\oint_C F \cdot dl = \iint_S \nabla \times F \cdot dS \tag{2.2}$$

$$\oint_C E \cdot dl = -\int_S \frac{\partial B}{\partial t} \cdot dA. \tag{2.3}$$

In general it can be said that the electromotive force, emf, can be described as

$$emf = \oint_C E \cdot dl \tag{2.4}$$

and by combining it with the magnetic flux, which can be written as

$$\Phi = \int_S B \cdot dA \tag{2.5}$$

the emf can be described as

$$emf = -\frac{\partial \Phi}{\partial t}. \tag{2.6}$$

This means that a magnetic field that links a circuit will induce a current inside the circuit. This is the reason for the behaviour of an transformer.

When an AC voltage is applied to a transformer a current will start to flow in the first winding. The current is then creating a magnetic field in the transformer which induces a current in the second winding. This can be seen in Figure 2.5.

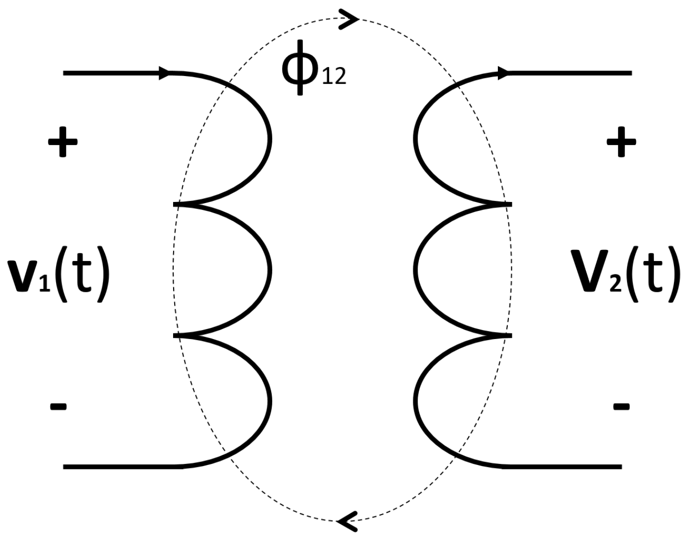

Figure 2.5: Setup for a transformer.

By using (2.5) the mutual flux, ϕ_{12}, can be expressed as the magnetic flux density through the surface of the second coil, S_2, see (2.7)

$$\Phi_{12} = \int_{S_2} B_1 \cdot ds. \tag{2.7}$$

The magnetic flux density is created by the current on the primary side, i_1 and can be described by Biot-Savart law as

$$B_1 = \frac{i_1 \mu_0}{4\pi} \oint_{C1} \frac{dl \times \hat{r}}{r^2} \tag{2.8}$$

where μ_0 is the permeability constant and r is the radius of the closed loop. From this equation it is possible to see that B_1 is proportional to the current on the primary side which gives that Φ_{12} is proportional to the same current and can be written as

$$\Phi_{12} = M i_1 \tag{2.9}$$

where M is the mutual inductance between the two sides of the transformer. By adding N_2 turns on the secondary side the flux linkage, Λ_{12}, can be expressed as

$$\Lambda_{12} = \Phi_{12} N_2 \tag{2.10}$$

and if combining this with (2.9), M can be expressed as in (2.11) in terms of Λ_{12} and i_1. M can also be described with Λ_{21} and i_2 which can be seen in (2.12).

$$M = \frac{\Lambda_{12}}{i_1 N_2} \tag{2.11}$$

$$M = \frac{\Lambda_{21}}{i_2 N_1} \tag{2.12}$$

The self inductance is expressed as the magnetic flux linkage per unit current in its loop, which can be written as

$$L_1 = \frac{\Lambda_{11}}{i_1}. \tag{2.13}$$

For a linear medium, the self inductance does not depend on the current. It depends on the geometrical shape, the physical arrangement of the conductor and the permeability of the medium. If M and the self inductances, for both the primary and the secondary coil, are obtained the coupling factor, k, can be calculated as

$$k = \frac{M}{\sqrt{L_1 L_2}}. \tag{2.14}$$

For an ideal transformer $k = 1$. This is due to that there will be no leakage flux which means that all flux that comes from the coil on the primary side will go through the coil in the secondary side. In this case L_1 and L_2 will be equal to M. A transformer in a conductive charger will consist of an iron core which means that k will be close to unity. However, the inductive charger will have a core of air which will decrease k heavily.

For an ideal transformer it is possible to transform parameters such as voltage, current and impedance from the secondary side to the primary side and vice versa.

This is done by using the turn ration of the transformer, see (2.15-2.17) for each case.

$$V_2' = V_2 \frac{N_1}{N_2} \tag{2.15}$$

$$I_2' = I_2 \frac{N_2}{N_1} \tag{2.16}$$

$$Z_2' = Z_2 \left(\frac{N_1}{N_2}\right)^2. \tag{2.17}$$

During real experiments there will always be a flux leakage in the transformer. In Figure 2.6 the equivalent circuit of a transformer can be observed.

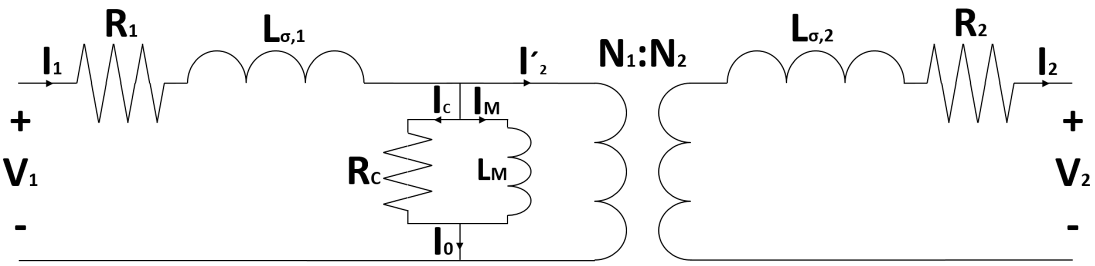

Figure 2.6: Equvalent circuit of a transformer.

The resistance R_1 and R_2 are the equivalent series resistances, ESR, for both of the coils and $L_{\sigma,1}$ and $L_{\sigma,2}$ are the leakage inductances for each coil.

2.3 Standards and Application

This section will provide the reader with some standards and information about charging and charging equipments for conductive charging. The information is based on [6]. It is possible to divide how an EV is charged in three separate categories, normal charging, semi-fast charging and fast charging. Normal charging is usually applied when charging an EV at home or at a place where the EV can be charged for 6 - 10 hours. The power for this case is around $2.3 - 3.7kW$ with a voltage level of 230 V. Only one phase is used in this case which means that the current level is between $10 - 16$ A. This is usually used at home which means that the EV can be charged during the night. Semi-fast charging means that the EV is charged for about 30 minutes up to a few hours. The power is around 3 - 5 times higher compared to the previous case which means that this type of charging is adapted for parking lots where the driver will be gone for the specified time. For example at the grocery store, at a cinema or a concert, etc. The third and last charging method is the fast charging. There is no definition on how fast this method has to be but usually the time should not exceed 20 minutes. The goal of this method is not to fully charge the EV but to extend the driving distance. In this case 50 kW, or more, is applied and after 20 - 30 min the capacity of the battery is around 80 %. With this method it is possible to charge an EV when taking a break during a longer trip or during more frequently driving in a city. When using fast charging DC is used instead of AC but companies are working on an AC solution as well.

To be able to connect the cable to the charging station and the EV an electrical connector, EC, is used in both ends of the cable. Sometimes the cable can be integrated into the charging station, in that case there is only a need for an EC between the cable and the EV. In 2014, the EU commission decided that the EC called Type 2 and Combo 2 should become standard for AC and DC respectively, for entire Europe [7][8]. But due to that some charging stations where installed before that announcement, a change of EC might not have been done. It is also important to state that this is just in Europe which means that the EC can be of another type in the rest of the world. Therefore the most common EC will be introduced.

The standard EC that is used at home is called Schuko which can provide with 16 A one phase. This EC can be used for charging an EV but it is not recommended due to that the Schuko is not designed to transfer high amounts of power during longer periods. If so, the EC can catch fire. Also, the Schuko does not have any communication pins, COM-PINs, which means that the Schuko does not have any communication with neither the charging station nor the EV. One EC that can transfer high power levels is the CEE connector. This EC is mostly used in industries and can handle 16 A for one phase. It can also handle much higher currents for three phases, but due to that the CEE does not have any COM-pins, as well as the Schuko, it is not recommended to charge an EV with it. The Schuko and the CEE are quite old fashioned and works well for equipment that does not need a communication link. Due to that communication is important when charging an EV, for safety reasons, more advanced EC has been used when charging stations have been installed. Examples of ECs that have COM-pins are, Type 1, Type 2, CHAdeMO and Combo 2.

Type 1, also known as Yazaki or SAE J1772, is designed for 32 A single phase and is installed for some cars today. But due to that it is only designed for single phase it is not an optimal option. Type 2, which is standard in Europe today, can handle both single phase and three phase with a current of 70 A and 63 A respectively. Unlike Type 1 and 2, CHAdeMO uses DC with a power of 50 kW. It can handle 500 V and currents up to 120 A. Due to the high power level CHAdeMO is equipped with eight COM-pins. The COM-pins are used to make sure that the connection of the EC is correct as well as checking the status of the cable and make sure that it is isolated. When this is done the battery in the EV is charged to about 80 % and when this value is reached the battery is charged with less power to ensure that the battery will not be damaged. The communication for the CHAdeMO is quick, around 200 ms, just to make sure that the battery is not charged with too high currents which may damage the battery. To make sure that one EC can handle both charging with AC and with DC(fast charging), Combo 2 was developed. It is also known as CCS and this EC consists of two contacts, one for normal and semi-fast loading, and one for fast charging. It is possible to say that Combo 2 is a Type 2 with fast charging and from the Type 2 it gets its COM-pins. The Combo 2 has, as well as Type 2, been classified as a standard for charging EVs in Europe but Combo 2 has also been developed in USA. The American version uses a Type 1 instead of Type 2 but due to that Combo 2 has become global most car companies has decided to use this in their cars.

There are also some companies that has developed there own EC, for example Renault with their Chameleon which has a rectifier inside the EV instead of having it in the charging station. When placing it inside the EV it has the possibility to use regenerative breaking as was mentioned before. By placing the rectifier in the car it is possible to make the charging station smaller as well as the conductive cable.

When charging an EV there are four so called modes, Mode 1 - 4, which represents different safety levels during charging of an EV. The four modes are represented in Figure 2.7. For Mode 1 it can be seen that there is no communication between the EV and the charging station. In this mode a Schuko or a CEE is used for single phase and three phase, respectively. It is recommended to use a current level of 10 A, for safety reasons, but as mentioned before it can handle 16 A. The reason for this is due to the lack of communication which means that the equipment is not protected against overheating or ground fault.

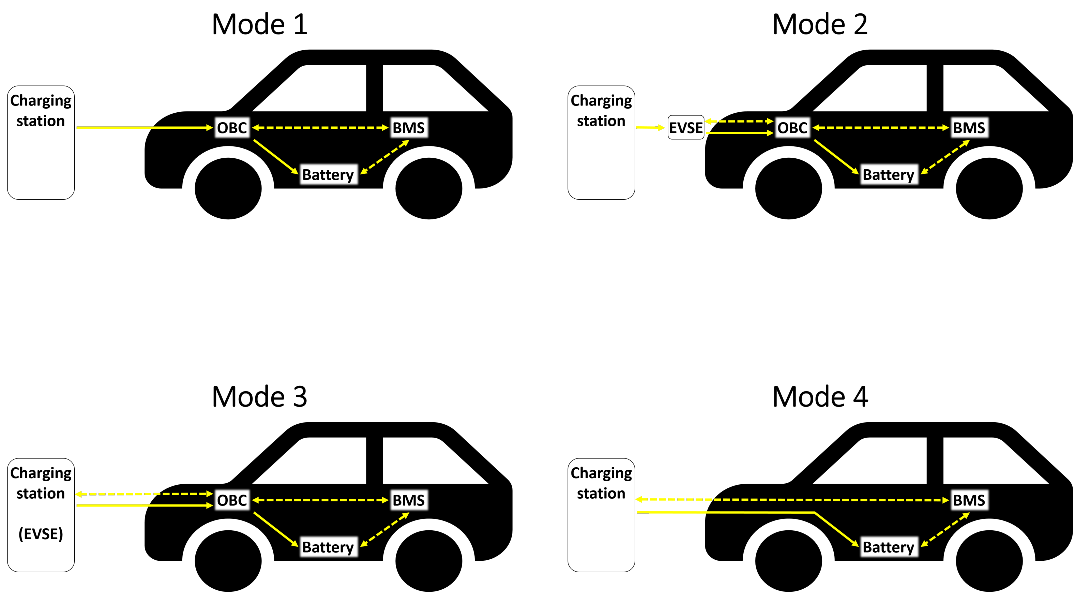

Figure 2.7: The different safety levels. The path of the power is represented by bold arrows and the communication path is represented by the dashed arrows.

For Mode 2 it can be seen that an electric vehicle supply equipment, EVSE, has been added between the car and the charging station. This mode can handle 32 A but it is important to make sure that the chosen EC can handle the high current as well. To establish a communication link between the EVSE and the EV a Type 1 or Type 2 EC is used. Due to that there is only a communication link between the EVSE and the EV, faults that occur at the outlet will not be handled. The EVSE must at least be able to make sure that the EV is connected in a proper way, monitor grounding and be able to turn on and off the power that is sent to the load. If these criteria are not fulfilled, the charging procedure will not start and if a fault is observed the power will be turned off. For Mode 3 the EVSE is now integrated in the charging station which means that the charging station is now handling the charging procedure. It can now handle 230 V and 400 V and currents up to 63 A which means that fast charging is now available, if the OBC can handle it. An intelligent charging post or a wall box is making sure that the charging of the EV is performed in a correct way by communicating with it continuously. The EV is connected to the cable via a Type 1 or Type 2, the cable itself is either integrated into the charging station or connected by a Type 2. The criteria are the same as for Mode 2, but due to that the charging station is communicating with the EV continuously, Mode 3 is the safest of the four modes. Mode 4 refers to fast charging, with DC, and as can be seen the charging station is now connected to the battery in the EV. The power level for this mode can be between 20 kW and 125 kW and the battery charging station is now communicating with the battery management system, BMS. The BMS is controlling the power level and how long time the battery can be charged. The criteria for shutting on and off are the same as for Mode 2 and 3.

3 Inductive Charging

Even if the concept of using inductive charging has been around since the dawn of Nikola Tesla it has only been used in the everyday life as a product for a couple of years. For example when it comes to recharging electrical toothbrushes. However, in recent years the so called Qi has been developed and become the standard for low power inductive charging. The most common way of using Qi is to charge low power object such as cellphones inductively using a high frequency. However, In May 2016 SAE International approved a standard for inductive charging for PH and EV. The standard is refereed to as SAE TIR J2954 and this can hopefully speed up the development of inductive charging for high power applications. The frequency that is specified for this standard is 85 kHz ($81.39 - 90$ kHz) and is for light duty vehicle systems. There are four classes of wireless power transfer, WPT, which are divided into different power levels. The classes are referred to as WPT 1-4 and the power levels are 3.7 kW, 7.7 kW, 11 kW and 22 kW respectively.

There has also been some research about inductive charging in Sweden. In 2015 Vattenfall started a research project, with several other companies, where 20 EVs were supposed to be charged wirelessly [9]. The power level was 3 kW with a voltage of 230 V. The wireless part consist of two coils, a primary and a secondary coil. The primary coil is placed on the ground and the secondary coil is placed under the luggage space. The secondary coil has the size of an A4 paper which is 210×297 mm^2.

As showed before, an inductive charging system contains of a similar setup as the conductive charging system. However, in this case the transformer is the interface between the charging system and the EV. This means that the rectifier, inverter and the coil on the primary side are placed outside the car and the secondary coil and the rectifier are placed inside the car. In Figure 3.1 a simple topology of the system can be seen where the dashed line shows which parts belongs inside of the car and which parts that belongs outside of the car. It can be seen that two compensation blocks has been added and the reason for this is due to the low amount of transferred active power. Compensation will be discussed more in the next section.

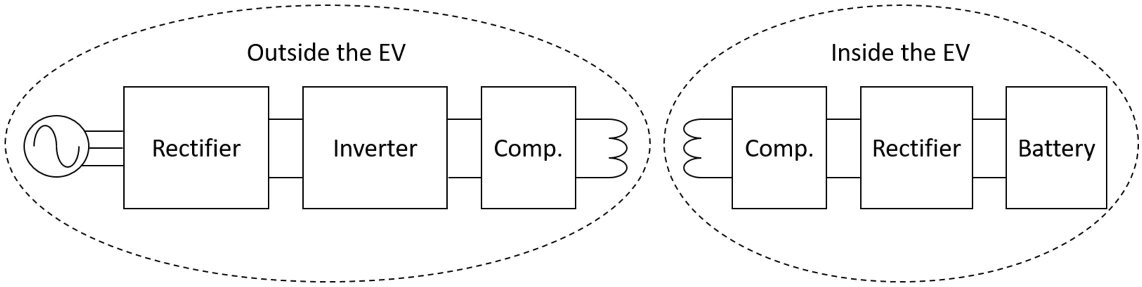

Figure 3.1: Block diagram of inductive charging.

It is usually desired to improve the system by adding a boost converter, like in the conductive case, to increase the power factor. It is also possible to add the boost converter inside the car. Adding power electronics inside the car will not only contribute to a higher power factor but can also contribute to a more efficient charging system. However, as in the case with the conductive charger there is a balance between the size and the performance of the charger.

3.1 Compensation

Compensation is used to maximise the active power on the output of a circuit by reducing the reactive power. The reason for why compensation must be applied during inductive charging is because the transformer has a much higher leakage inductance compared to the transformers that are used for conductive charging. This can be done by placing capacitors in series or in parallel on both the primary and the secondary side of the transformer. When compensating on the primary side a more stiff voltage source will occur which makes the power transfer more effective. Due to that both sides can be compensated either in series, S, or parallel, P, a total amount of four topology combinations can be obtained, SS, SP, PS and PP [10].

The first topology that will be introduced is the SS compensation, see Figure 3.2. By using a matching capacitance on the primary side the imaginary part of the impedance will be zero which means that the voltage on the primary winding will be equal to V_1.

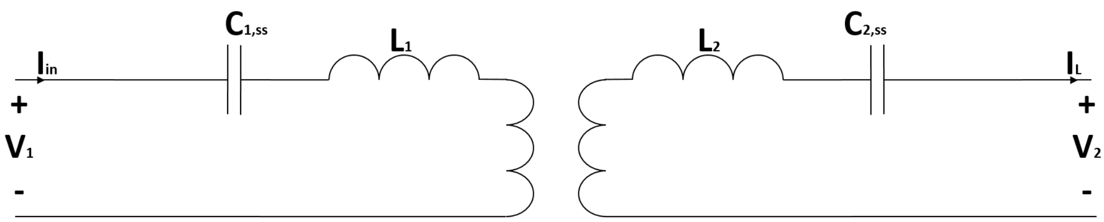

Figure 3.2: Series compensation on both the primary and the secondary side.

The total impedance on the primary side can then be expressed as

$$Z_{1,ss} = j\omega L_1 + \frac{1}{j\omega C_{1,ss}}. \tag{3.1}$$

To achieve zero impedance on the primary side the size of the capacitance can be selected as

$$C_{1,ss} = \frac{1}{\omega^2 L_1}. \tag{3.2}$$

For the capacitance, $C_{2,ss}$, on the secondary side, the expression will look the same but with the inductance L_2 instead. The imaginary part of the impedance on both sides are now equal to zero which means that the active power will now be equal to the apparent power. If a load is attached on the output the load would see the transformer as a current source which means that the load current is independent of the load.

By keeping the capacitance on the primary side in series and place the capacitance on the secondary side in parallel with the load, the transformer now acts as a voltage source instead. This can be seen in Figure 3.3. The output current will now be a little bit smaller than the current through the winding on the secondary side due to that the current will now also go through the capacitor $C_{2,sp}$. The size of the capacitance can be expressed in the same way as for the SS topology but it can also be expressed with the coupling factor, k, to eliminate the reactive power provided from the input voltage source. The expression for $C_{2,sp}$ will be the same as before but the expression for $C_{1,sp}$ will then be

$$C_{1,sp} = \frac{1}{\omega^2 L_1 \cdot (1 - k^2)}. \tag{3.3}$$

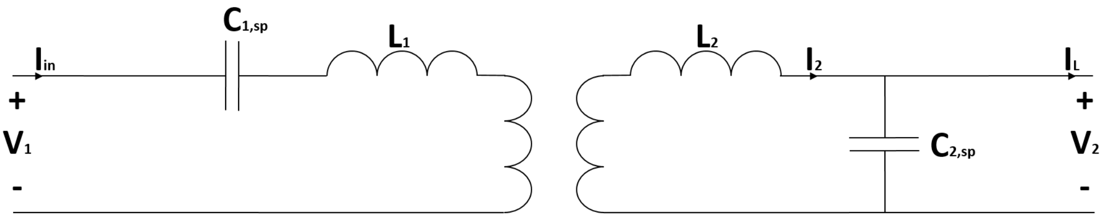

Figure 3.3: Series compensation on the primary side and parallel compensation on the secondary side.

By swapping the two capacitors with each other the PS topology is achieved. Here, as can be seen in Figure 3.4 an extra inductance $L_{in,ps}$ needs to be added as the interface between the input and the parallel capacitance. This is due to that the circuit is feed with a current source. The added inductance should be equal to L_1 and the capacitors are calculated as before. The system will act as a voltage source in this case as well.

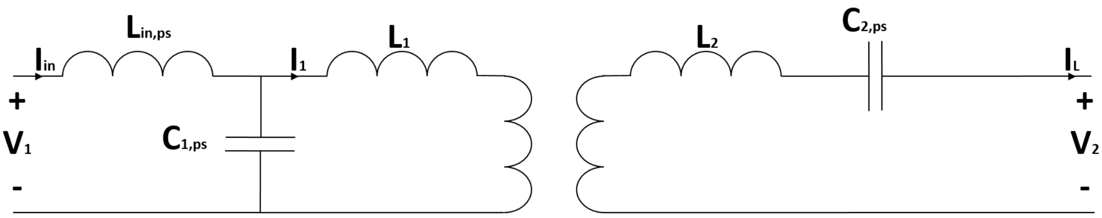

Figure 3.4: Parallel compensation on the primary side and series compensation on the secondary side.

The last topology is the PP topology, see Figure 3.5. As in the previous case an extra inductance needs to be added between the voltage source and $C_{1,pp}$ but this inductance needs to be expressed with k as

$$L_{in,pp} = L_1(1 - k^2). \tag{3.4}$$

Also, $C_{1,pp}$ need to be expressed as in the case with SP compensation. $C_{2,pp}$ will be expressed as before and $C_{1,pp}$ is expressed as

$$C_{1,pp} = \frac{1}{\omega^2 L_1 \cdot (1 - k^2)}. \tag{3.5}$$

Due to the position of $C_{1,pp}$ and $L_{in,pp}$ a current source is created and the transformer will then be fed with a constant current. This allows the system to act as a current source.

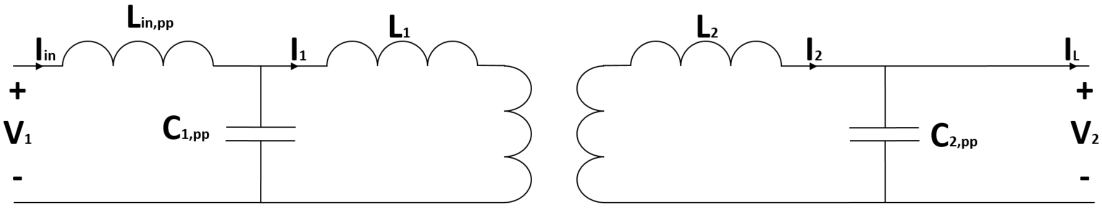

Figure 3.5: Parallel compensation on both the primary and the secondary side.

3.2 Ferrite bars

To be able to concentrate the magnetic flux in the coils ferrite bars are usually placed on the outside of the transformer. The ferrite bars have a high permeability, μ, which means that the magnetic flux will be concentrated into this material. By concentrating the magnetic flux, the leakage can be heavily reduced which means that the coupling between the two coils will increase. In Figure 3.6 two coils without ferrite bars is showed in a 2D-axisymmetric geometry. The lower coil is fed with an AC-current which creates a pulsating magnetic field that will induce a current in the upper coil, as explained in the previous chapter. The magnetic flux is transferred from the lower coil to the upper one. However, a lot of the flux is distributed around the lower coil which means that there is a lot of leakage flux. This leakage flux can interfere and damage other components that are placed nearby. Also, it is important to keep the magnetic flux away from humans, and other animals. This is due to that the magnetic flux can be dangerous if exposed frequently or during long periods. It can also induce currents in metal objects like rings and watches which can cause burn damages.

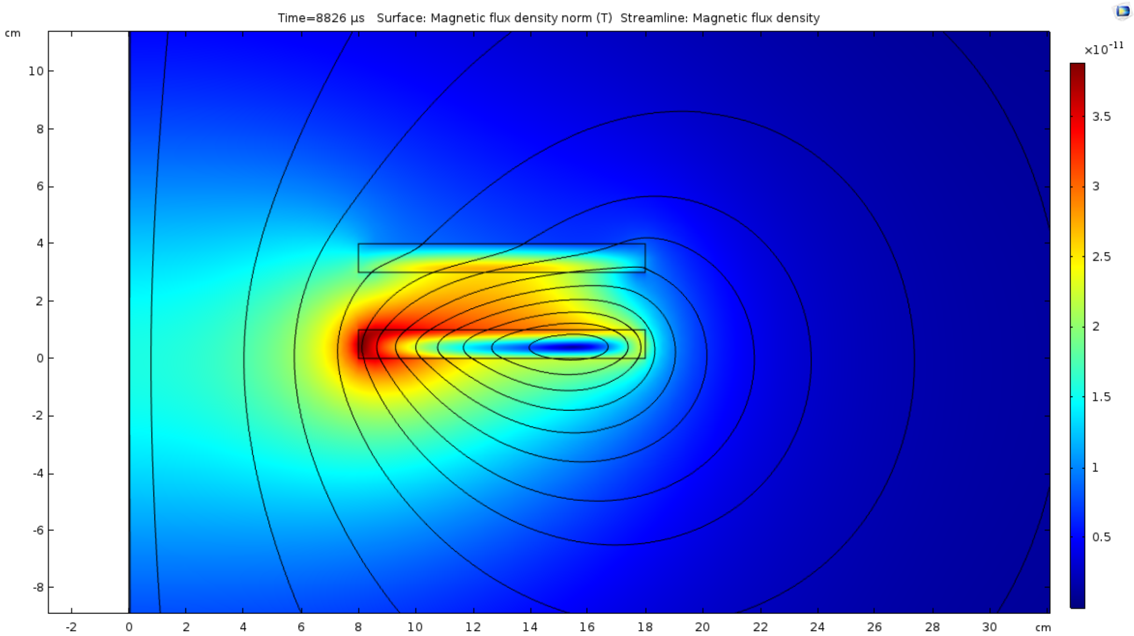

Figure 3.6: Two coils without ferrite bars. The leakage flux is high for this case.

As mentioned before, the ferrite bars are placed on the outside of the coils and due to the high permeability, the magnetic flux density will be concentrated into the ferrite bars. By looking at Figure 3.7 it can be seen that the leakage flux is now reduced.

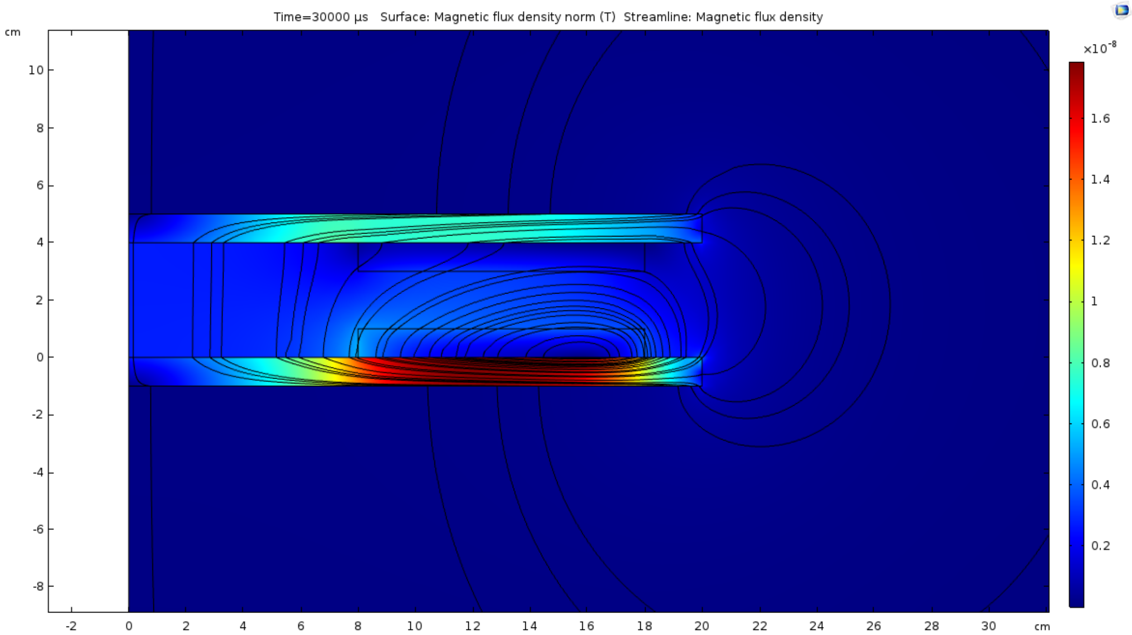

Figure 3.7: Two coils with ferrite bars. The leakage flux is low for this case.

The reason for why ferrite bars are used instead of for example iron, which also have a high μ_r is because iron is a much better conductor. This means that eddy currents will be induced in the iron which will provide with losses in the transformer. To be able to reduce the cost for the ferrite bars it is not needed to cover the entire coil with ferrite bars, a smart and well planed structure can reduce the amount of ferrite bars and still keep the same performance. Due to that the coils are already designed different placements for the ferrite bars will not be tested but due to that a cost analysis of the entire system will be made it is important to not use more ferrite bars than needed.

4
Methods (Power Electronic)

The charging setup that will be simulated consists of a boost converter and a DC/DC step. The conductive charging setup was designed for three different cases for the output, low voltage and high current, medium high voltage and medium high current and last high voltage and low current. All three cases where designed to provide with 3.3 kW and can be referred to as Case 1, Case 2 and Case 3, respectively. More specific information about the voltages and currents for the different cases can be seen in Table 4.1. Where V_{in} is the input voltage, $I_{in,max}$ is the maximum input current, V_{DC} is the voltage that is applied to the inverter and V_0 and I_0 is the output voltage and current.

Table 4.1: Specifications for the three cases.

Parameter	Case 1	Case 2	Case 3
V_{in}	230 V	230 V	230 V
$I_{in,max}$	16 A	16 A	16 A
V_{DC}	450 V	600 V	450 V
V_0	100 V	450 V	600 V
I_0	33 A	7.33 A	5.5 A

The inductive charging setup that will be simulated will consist of a boost converter and a DC/DC step. The boost converter will have the same design as in the conductive cases. The DC/DC step consists of only one design layout, this was due to that an already prebuilt design existed and to make fair comparisons the values for the transformer was used. The rest of the components were designed with respect to the transformer. The DC/DC step was simulated with an input voltage of 450 V and it is supposed to deliver 3.3 kW, as the conductive setup. All simulations were made in LTspice IV. The following section will first introduce the design of the boost converters. After that the design of the DC/DC step for the three different cases of conductive charging will be presented. Last, the design of the inductive charging setup will be introduced.

4.1 Boost AC/DC converter in PFC application

To be able to use the high frequency converter the power from the grid must first be rectified. This is done by using a rectifier which consists of four diodes which gives that output will always supply with a positive voltage and a positive current.

The rectifier is then connected to a boost converter which consists of an inductance, a switch and a diode. The chosen diode is a DSEI2x101-12P with a repetitive reverse voltage of 1200 V and a reverse recovery time of 40 ns. When the diode is conducting the voltage drop over the diode is 1.61 V. The diode can withstand a forward current of 91 A. The switch is a MOSFET called IPW65R037C6 and in Table 4.2 the most important ratings of the MOSFET can be seen. This MOSFET was chosen due to its low resistance which means that the conduction losses will be low. It is also wanted that the parasitic output capacitance C_{oss} is low. The reason for this will be explained in the next section where zero voltage switching will be explained.

Table 4.2: ratings of the IPW65R037C6.

IPW65R037C6	
Parameter	Value
V_{DS}	700 V
R_{DS}	37 mΩ
$I_D(T = 25°C)$	83.2 A
$I_D(T = 100°C)$	52.6 A
C_{oss}	380 pF

The switching frequency for the boost was chosen to be less than half of the switching frequency of the inverter and due to that 85 kHz is standard for inductive charging this was chosen to be used for the inverter for conductive charging cases as well. So the switching frequency for the boost converter was chosen to be 35 kHz. The inductance can then be calculated as

$$L_{CCM} = \frac{V_{DC}}{4f_{sw}\Delta I_L} \tag{4.1}$$

where ΔI_L is the current ripple through the inductor, peak-to-peak. The maximum current that the inductor have to withstand is $\sqrt{2}I_{in,max} = 22.6\ A$ and with a $\Delta I_L = 0.2\sqrt{2}I_{in,max}$ the inductance can be calculated as

$$L_{CCM,1} = \frac{450\ V}{4 \cdot 35\ kHz \cdot 4.52\ A} = 711\ \mu H \tag{4.2}$$

$$L_{CCM,2} = \frac{600\ V}{4 \cdot 35\ kHz \cdot 4.52\ A} = 948\ \mu H \tag{4.3}$$

$$L_{CCM,3} = \frac{450\ V}{4 \cdot 35\ kHz \cdot 4.52\ A} = 711\ \mu H \tag{4.4}$$

for the three cases. $L_{CCM,1}$ and $L_{CCM,3}$ was set to 700 μH which gives a current ripple of 4.59 A and $L_{CCM,2}$ was set to 950 μH which gives a current ripple of 4.51 A. According to [11], the output capacitance can be calculated as

$$C_0 = \frac{P_0}{2\omega V_{DC}\Delta V_{DC}} \tag{4.5}$$

and it is desired to cancel out as much voltage ripple as possible due to that the DC/DC step should be fed with a DC signal [11]. Therefore a output capacitance of 100 μF was chosen. The calculated voltage output ripple is then calculated to be

$$\Delta V_{0,1} = \frac{3300\ W}{2 \cdot 2 \cdot \pi \cdot 35\ kHz \cdot 450\ V \cdot 100\ \mu F} = 0.167\ V \tag{4.6}$$

$$\Delta V_{0,2} = \frac{3300\ W}{2 \cdot 2 \cdot \pi \cdot 35\ kHz \cdot 600\ V \cdot 100\ \mu F} = 0.125\ V \tag{4.7}$$

$$\Delta V_{0,3} = \frac{3300\ W}{2 \cdot 2 \cdot \pi \cdot 35\ kHz \cdot 450\ V \cdot 100\ \mu F} = 0.167\ V \tag{4.8}$$

The duty cycle, D, for an ideal boost converter can be calculated as

$$D = 1 - \frac{V_{in}}{V_0}. \tag{4.9}$$

It is important to make sure that D is not too close to 1. This is due to that the gain will quickly decay due to parasitic elements that is neglected in (4.9). D for all three cases are calculated to be

$$D = 1 - \frac{230\ V}{450\ V} = 0.489 \tag{4.10}$$

$$D = 1 - \frac{230\ V}{600\ V} = 0.617 \tag{4.11}$$

$$D = 1 - \frac{230\ V}{450\ V} = 0.489. \tag{4.12}$$

As can be noticed the boost converter for Case 1 and Case 3 are exactly the same. This is due to that the input and the DC-voltage is the same for both cases as can be seen in Table 4.1.

4.2 DC/DC Converter for Conductive Charging

The DC/DC converter consists of an inverter, a transformer and a rectifier, as was mentioned before. The inverter consists of four MOSFETs, the MOSFETs are the same as the MOSFET that was used in the boost converter. The inverter will convert the DC-signal, from the boost converter, into an AC-signal which will go through the transformer and after that it will be rectified again and connected to a load which in this case is a simplification of a battery. The same inverter is used for all three cases, the only thing that is changed for the inverter is the control settings for the gate pulses. The switching frequency is set to 85 kHz which is, as mentioned before, standard for inductive charging and will also be the frequency that will be used for the combined setup.

At high frequency application there will be high switching losses. To be able to reduce these losses the inverter will be using zero voltage switching, ZVS, which means that current will not start to flow through the MOSFET until the voltage across it has reached zero. This is done by using an anti-parallel diode that every MOSFET is equipped with together with the resonant capacitance, C_R, which is depending on the parasitic output capacitance C_{oss} and the transformer capacitance C_T. ZVS is achieved when the magnetic energy in the inductor is larger than the electrical energy in the capacitor, this means that the capacitor will be discharged at every off-state each switching period. This condition can be expressed as

$$\frac{I^2 L}{2} > \frac{V_{DC}^2 C_R}{2}. \tag{4.13}$$

It can be noticed that to be able to fulfil this criteria it is important to keep C_{oss} low when using high voltages across the MOSFET otherwise an extra inductance might be needed to add to fulfil the criteria. It is also important to make sure that the design can handle low power levels because low power levels means low I. The results of using and not using ZVS can be seen in Figure 4.1 and 4.2, respectively. In the first figure it can be seen that the voltage over the MOSFET has reached zero before the current get positive which is not the case in the second figure. This means that for low D, a current will flow through the MOSFET at the same time as there is a voltage over the MOSFET. This means that the switching losses will be high for low D.

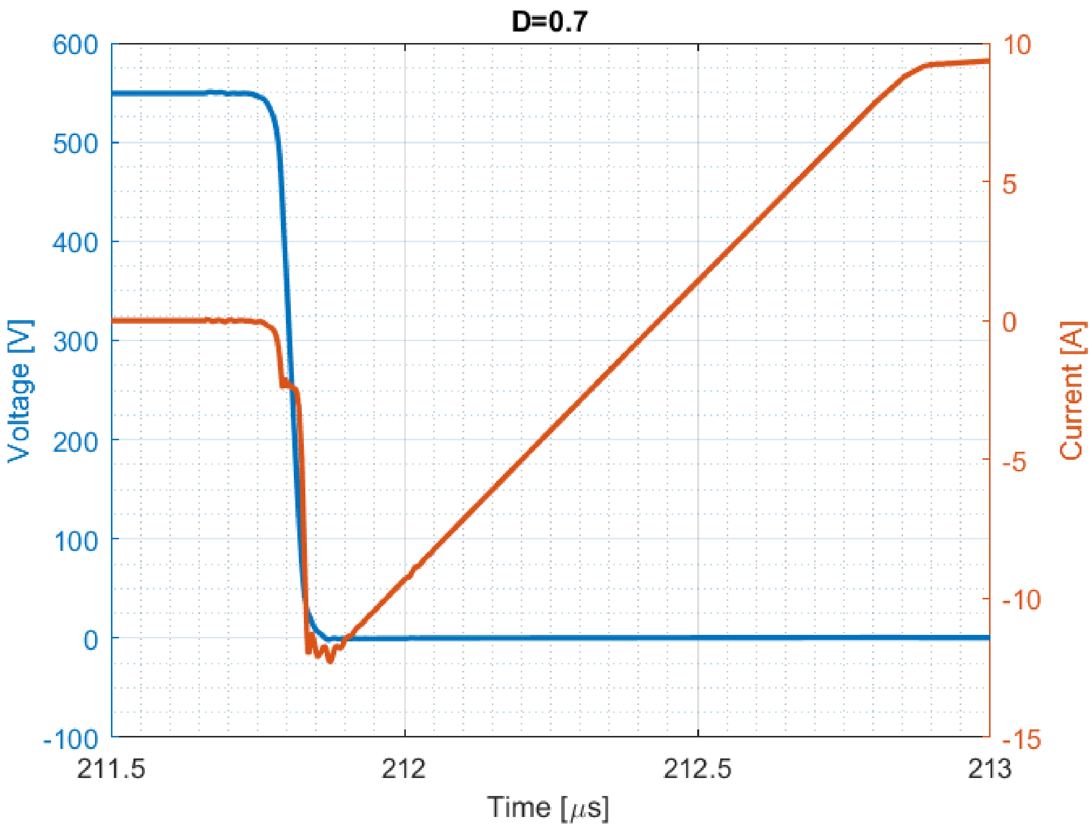

Figure 4.1: Voltage over the MOSFET and the current through the MOSFET at turn on when ZVS is achieved.

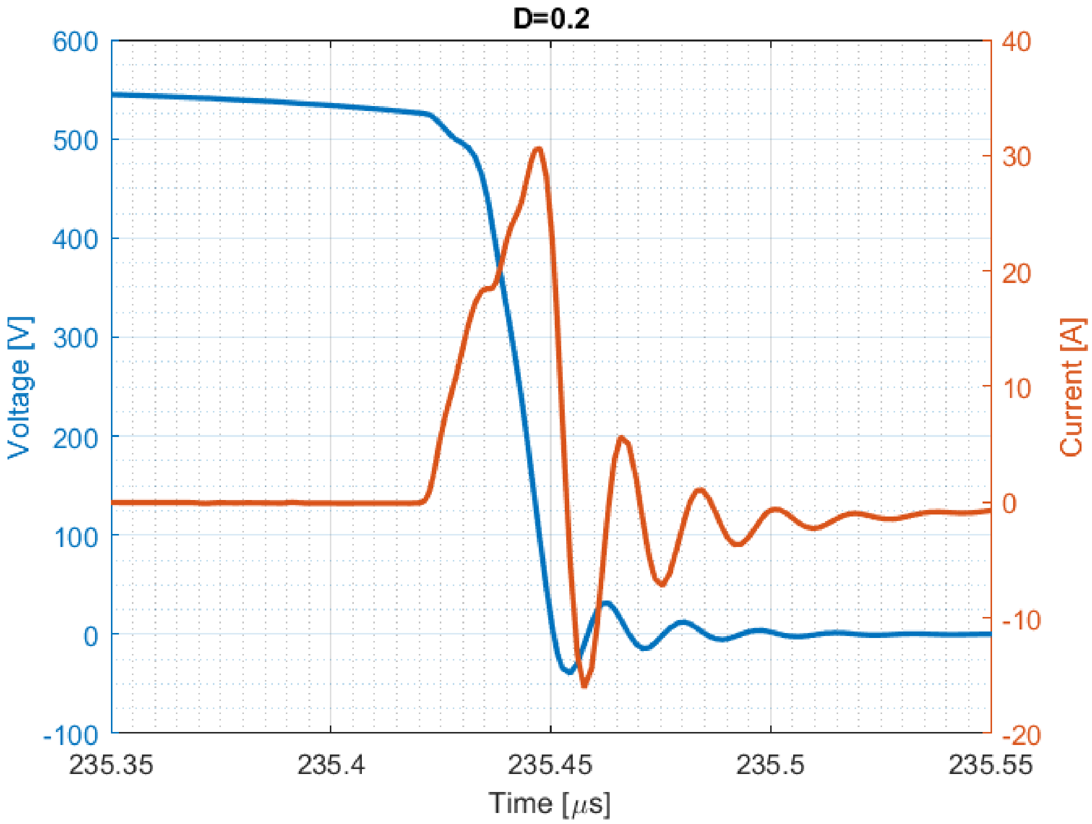

Figure 4.2: Voltage over the MOSFET and the current through the MOSFET at turn on when ZVS is not achieved.

The inverter will also be using phase shift control which means that the gate signals will be phase shifted. The phase shift is in this case refereed to as the time between when MOSFET-3 is turned on and MOSFET-1 is turned on. This is the same as the time between when MOSFET-4 is turned on and MOSFET-2 is turned on. The phase shift of the gate signals can be seen in Figure 4.3. There is also a small delay between when MOSFET-1 is turned off and MOSFET-2 is turned on, as well as for MOSFET-3 and MOSFET-4. By introducing this small delay each MOSFET will now be turned off and turned on at specific times which will prevent short circuits in the legs of the inverter. By controlling the phase shift, D will be controlled as well, by looking at the figure it can be seen that when MOSFET-1 and MOSFET-3 is on the output signal will be positive and when MOSFET-2 and MOSFET-4 is on the output signal is negative. The amplitude of the output signal will always be equal to the DC voltage that the inverter is fed with, in this case 450 V. However, the rms value of the signal is affected by the phase shift. By increasing the phase shift D will decrease.

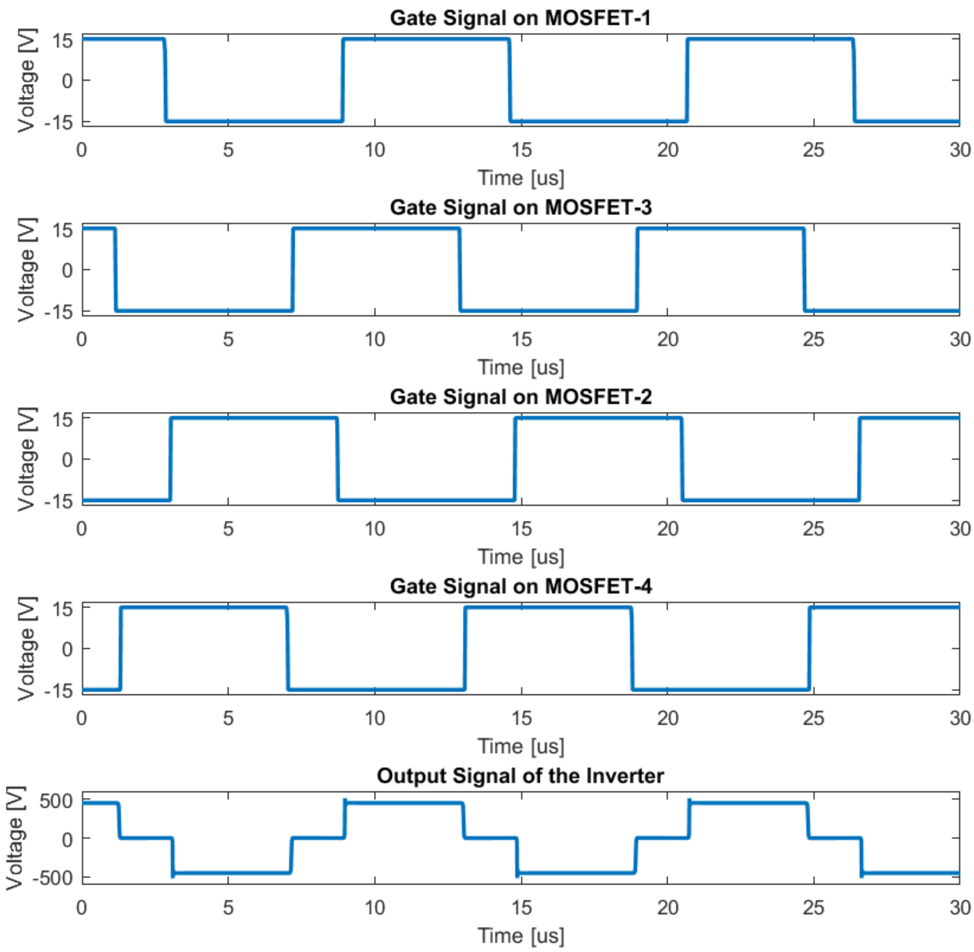

Figure 4.3: Gate signals for all MOSFETs and the output signal of the inverter

The effective duty cycle of the inverter can be calculated as

$$D = \frac{V_0}{V_{DC}} n \tag{4.14}$$

where n is the turn ratio of the transformer. It is preferable that the maximum value of D should never exceed 0.8. This means that n has to be chosen differently for each case so D will become smaller than 0.8. D was calculated for each case to be

$$D_1 = \frac{100\ V}{450\ V} \cdot \frac{13}{4} = 0.722 \tag{4.15}$$

$$D_2 = \frac{450\ V}{600\ V} \cdot \frac{14}{15} = 0.7 \tag{4.16}$$

$$D_3 = \frac{600\ V}{450\ V} \cdot \frac{5}{9} = 0.74. \tag{4.17}$$

The equivalent capacitance of the resonant tank can be expressed as

$$C_R = \frac{8}{3}C_{oss} + C_T \tag{4.18}$$

where C_{oss} is 380 pF, which was given earlier in Table 4.2. The factor $\frac{8}{3}$ is an approximation due to that during each transition two switches are always involved and the values of these capacitors are never constant [4]. The transformer capacitance, C_T is assumed to be 10 pF in this case. The capacitance of the resonant tank is then calculated to be 1023 pF.

When designing the transformer it is important to make sure that the desired voltage and current on the output is achieved. It is also important to make sure that the connection between the two coils are good and that a sufficiently leakage inductance is used to reach resonance in the circuit. To be able to calculate the parameters for the transformer the current output ripple ΔI_0 needs to be calculated. It can be expressed as

$$\Delta I_0 = \frac{V_0(1-D)}{4L_f f_{sw}}. \tag{4.19}$$

Where L_f is the output inductor. Here L_f is chosen so ΔI_0 will be approximately $0.1 I_0$ for all three cases. ΔI_0 will then be calculated to be

$$\Delta I_{0,1} = \frac{100\ V \cdot (1-0.722)}{4 \cdot 25\ \mu H \cdot 85\ kHz} = 3.27\ A \tag{4.20}$$

$$\Delta I_{0,2} = \frac{450\ V \cdot (1-0.7)}{4 \cdot 500\ \mu H \cdot 85\ kHz} = 0.79\ A \tag{4.21}$$

$$\Delta I_{0,3} = \frac{600\ V \cdot (1-0.74)}{4 \cdot 900\ \mu H \cdot 85\ kHz} = 0.51\ A. \tag{4.22}$$

The magnetizing inductance, L_M can be expressed as

$$L_M > \frac{nDV_{DC}}{4\Delta I_0 f_{sw}}. \tag{4.23}$$

It is important that L_M is big enough to make sure that the magnetization current is smaller than the current output ripple transformed to the primary side. L_M can be expressed as below for the three cases:

$$L_{M,1} > \frac{13}{4} \cdot \frac{0.722 \cdot 450\ V}{4 \cdot 3.27\ A \cdot 85\ kHz} = 949.7\ \mu H \tag{4.24}$$

$$L_{M,2} > \frac{14}{15} \cdot \frac{0.7 \cdot 600\ V}{4 \cdot 0.79\ A \cdot 85\ kHz} = 1459\ \mu H \tag{4.25}$$

$$L_{M,3} > \frac{5}{9} \cdot \frac{0.74 \cdot 450\ V}{4 \cdot 0.51\ A \cdot 85\ kHz} = 1067\ \mu H \tag{4.26}$$

and are set to 1000 μH, 1500 μH and 1100 μH respectively. L_M is in these cases refereed to the primary side of the transformer. The leakage inductance for the primary side is chosen so ZVS will be achieved for the three cases. To be able to reach ZVS (4.13) must be fulfilled. The electrical energy is calculated to be

$$W_{c,1} = \frac{1023\ pF \cdot 450\ V^2}{2} = 103.58\ \mu J \tag{4.27}$$

$$W_{c,2} = \frac{1023\ pF \cdot 600\ V^2}{2} = 184.14\ \mu J \tag{4.28}$$

$$W_{c,3} = \frac{1023\ pF \cdot 450\ V^2}{2} = 103.58\ \mu J. \tag{4.29}$$

for each case respectively. This means that the magnetic energy from the leakage inductance must be greater than the electrical energy, this inductance is referred to the primary side. The leakage inductance, L_σ can be expressed as

$$L_\sigma > \frac{2W_c}{I_p^2} \tag{4.30}$$

where I_p is the peak value of the primary current which is the sum of the magnetization current and the load current with its ripple transformed to the primary side, which can be seen in (4.31).

$$I_p = I_M + \frac{I_0 + \Delta I_0}{n} \tag{4.31}$$

I_M can be calculated with the following equation

$$I_M = \frac{DV_{DC}}{4L_M f_{sw}} \tag{4.32}$$

and for the three cases it is calculated to

$$I_{M,1} = \frac{0.722 \cdot 450\ V}{4 \cdot 1000\ \mu H \cdot 85\ kHz} = 0.955\ A \tag{4.33}$$

$$I_{M,2} = \frac{0.7 \cdot 600\ V}{4 \cdot 1500\ \mu H \cdot 85\ kHz} = 0.824\ A \tag{4.34}$$

$$I_{M,3} = \frac{0.74 \cdot 450\ V}{4 \cdot 1100\ \mu H \cdot 85\ kHz} = 0.890\ A. \tag{4.35}$$

It is important to make sure that ZVS is achieved for low power levels as well as high power levels. Therefore the transformer will be designed so that ZVS will be achieved for half of the nominal load. This means that the output current will be halved. This gives that I_p will be equal to

$$I_{p,1} = 0.955\ A + \frac{\frac{33}{2}\ A + 3.27\ A}{13/4} = 7.038\ A \tag{4.36}$$

$$I_{p,2} = 0.824\ A + \frac{\frac{7.33}{2}\ A + 0.79\ A}{14/15} = 5.597\ A \tag{4.37}$$

$$I_{p,3} = 0.890\ A + \frac{\frac{5.5}{2}\ A + 0.51\ A}{5/9} = 6.758\ A \tag{4.38}$$

for the three cases with half of the output power. The leakage inductance can then be calculated for each case as

$$L_{\sigma,1} > \frac{2 \cdot 103.58\ \mu J}{7.038\ A^2} = 4.18\ \mu H \tag{4.39}$$

$$L_{\sigma,2} > \frac{2 \cdot 184.14\ \mu J}{5.597\ A^2} = 11.75\ \mu H \tag{4.40}$$

$$L_{\sigma,3} > \frac{2 \cdot 103.58\ \mu J}{6.758\ A^2} = 4.54\ \mu H. \tag{4.41}$$

To make sure that ZVS will be applied for even lower power levels the leakage inductance was chosen to be $5\mu H$, $12\mu H$ and $5\mu H$ for each case respectively. By adding the leakage inductance and the mutual inductance the self inductance of the coils can be obtained. The self inductance for both the primary and the secondary side is expressed as

$$L_1 = L_{\sigma,1} + M \tag{4.42}$$

$$L_2 = L_{\sigma,2} + M. \tag{4.43}$$

Due to that the output signal will be a square wave where the output DC signal will be the average of the square wave. The DC signal can be expressed as

$$V_{DC} = \hat{V_2} D. \tag{4.44}$$

The inductance for the secondary side can be expressed as

$$L'_{M,1} = 1000\ \mu H \left(\frac{100\ V/0.722}{450\ V} \right)^2 = 94.733\ \mu H \tag{4.45}$$

$$L'_{M,2} = 1500\ \mu H \left(\frac{450\ V/0.7}{600\ V} \right)^2 = 1722.0\ \mu H \tag{4.46}$$

$$L'_{M,3} = 1100\ \mu H \left(\frac{600\ V/0.74}{450\ V} \right)^2 = 3571.1\ \mu H. \tag{4.47}$$

The mutual inductance can be calculated as

$$M = \frac{L_M}{DV_1/V_2} \tag{4.48}$$

and for the three cases they are calculated to

$$M_1 = 1000\ \mu H \frac{100\ V}{0.722 \cdot 450\ V} = 307.8\ \mu H \tag{4.49}$$

$$M_2 = 1500\ \mu H \frac{450\ V}{0.7 \cdot 600\ V} = 1607\ \mu H \tag{4.50}$$

$$M_3 = 1100\ \mu H \frac{600\ V}{0.74 \cdot 450\ V} = 1982\ \mu H. \tag{4.51}$$

For the three cases, $L_{\sigma,2}$ is assumed to be 2 μH, 3 μH and 4 μH, respectively. These assumptions are based on the amount of turns on the secondary side and the size of the inductors on the secondary side. Compared to $L_{\sigma,1}$, which contributes with ZVS, $L_{\sigma,2}$ is just a parasitic component and it is desired to keep it as low as possible. It might be possible to have an even lower $L_{\sigma,2}$ but it will not be brought up in this report. As mentioned before an ideal transformer will have $k = 1$ but due to that leakage inductance has been added this is not the case anymore. However, k for high frequency transformer that is used in a conductive charger usually is around 0.99 or above. For the three cases, k be calculated with (2.14) as

$$k_1 = \frac{307.8\ \mu H}{\sqrt{(5\ \mu H + 1000\ \mu H) \cdot (2\ \mu + 94.733\ \mu)}} = 0.9872 \tag{4.52}$$

$$k_2 = \frac{1607\ \mu H}{\sqrt{(12\ \mu H + 1500\ \mu H) \cdot (3\ \mu H + 1722.0\ \mu)}} = 0.995 \tag{4.53}$$

$$k_3 = \frac{1982}{\sqrt{(5\ \mu H + 1100\ \mu H) \cdot (4\ \mu H + 3571.1\ \mu)}} = 0.9972. \tag{4.54}$$

As can be seen the coupling factor is close to one in all three cases. However, it is usually desired to have k above 0.99 which it not the case for k_1.

To represent the conduction losses in the winding of the high frequency transformer a equivalent series resistance, ESR, needs to be added. These are also assumed due to that the thickness and length of the wire is unknown. The amount of turns is known and therefore the ESR is assumed to be linearly dependent on the amount of turns. It is assumed that one turn provides with 10 $m\Omega$ which therefore provides with the following ESR for both the primary and the secondary side. So for the three cases, the ESR for the primary side is then calculated to be 130 $m\Omega$, 140 $m\Omega$ and 50 $m\Omega$ and the ESR for the secondary side is calculated to be 40 $m\Omega$, 150 $m\Omega$ and 90 $m\Omega$, respectively.

The output current ripple was calculated earlier when L_f was decided but it is also necessary to calculate and minimise the output voltage ripple, ΔV_0 as well. It is reduced by adding a capacitor at the output, as for the boost converter, and can be expressed as

$$C_{out} \geqslant \frac{\Delta I_0}{16 \cdot f_{sw} \Delta V_0}. \tag{4.55}$$

For a voltage ripple of 1 V, for all three cases, the output capacitance are calculated to be

$$C_{out,1} \geqslant \frac{3.27\ A}{16 \cdot 85\ kHz \cdot 1\ V} = 2.40\ \mu F \tag{4.56}$$

$$C_{out,2} \geqslant \frac{0.79\ A}{16 \cdot 85\ kHz \cdot 1\ V} = 0.580\ \mu F \tag{4.57}$$

$$C_{out,3} \geqslant \frac{0.51\ A}{16 \cdot 85\ kHz \cdot 1\ V} = 0.375\ \mu F. \tag{4.58}$$

The value of capacitors are set to 3 μF, 1 μF and 1 μF, respectively. By using a low value for the output capacitor the time constant can be kept low. This will reduce the simulation time heavily. However, a bigger capacitance can be chosen for a real setup. A bigger capacitance will require more space and will probably be more expensive.

4.3 Setup for inductive charging

As mentioned before, the topology for an inductive charging system looks quite the same as the topology of a conductive charging system. This means that some components from the conductive charging systems will be used in the inductive charging system as well and some components needs to be adjusted a bit. The combined system is assumed to be a compromise between the two systems. Therefore it is important to make sure that the difference between the components for the inductive charging system is small compared to the components for the conductive charging system. Therefore, the same inverter with the same MOSFETs will be used.

For inductive charging, k, will be much lower than for conductive charging and is now depending on the distance between the primary and the secondary coil. Misalignment between the coils will also change the value for k. For inductive charging k is usually around 0.2 and due to the low k, the leakage inductance is much higher than for conductive charging. This means that ZVS can be achieved with a much lower current but at the same time the flux leakage will be much higher. To make sure that as much active power as possible is transferred a compensation must be added on both sides of the transformer. The mutual inductance between the two coils are depending on the distance between the coils and due to that one coil is placed inside the EV and one on the ground the distance between them may vary each time the EV is charged. This gives that k is depending on the distance between the coils. Therefore, an SS topology is chosen where the value of the capacitors are not depending on the coupling factor. The values of the capacitors are calculated to be

$$C_{SS} = \frac{1}{L\omega^2} = \frac{1}{214\ \mu H \cdot (2\pi \cdot 85\ kHz)^2} = 16.38\ nF. \tag{4.59}$$

However, it is usually desired to use several small capacitors in parallel and in series instead of using one big capacitance. By connecting the capacitors in parallel it is possible to split up the current which means that each capacitor will have to withstand a lower temperature. By connecting them in series the capacitor bank can withstand higher voltages. It is important to state that the voltage drop over the capacitance can be much higher than the input voltage. A general topology of the capacitor bank can be seen in Figure 4.4 and the total capacitance of the capacitance bank can be expressed as

$$C_{tot} = \frac{C_{cap}N}{M} \tag{4.60}$$

where C_{cap} is the capacitance for one capacitor, N is the number of capacitors in parallel and M is the number of capacitors in series.

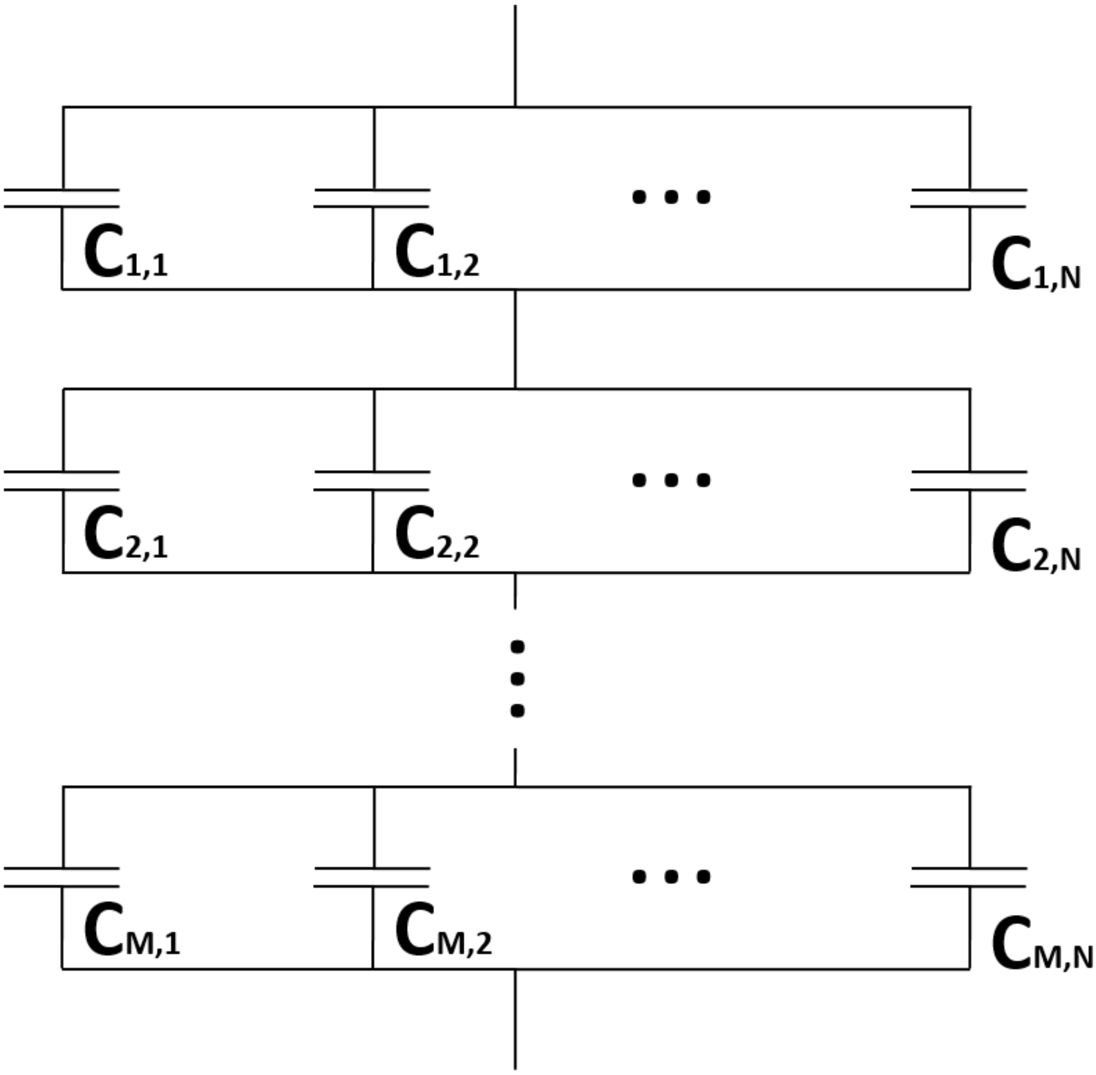

Figure 4.4: General topology for a capacitor bank.

These capacitor banks will be treated as one capacitor during the simulations but for the cost analysis several small capacitors will be used to create a capacitor that represents 16.38 nF.

As mentioned before, the voltage drop over the capacitor is needed to determine how many capacitors that is needed in series. During the simulations the voltage drop over both capacitors was measured. For the primary side the peak voltage was 1.688 kV and for the secondary side the peak voltage was measured to be 2.528 kV. The chosen capacitor is a polypropylene film capacitor with AC voltage rating of 1.5 kV and its capacitance is 3.3 nF. This gives that the capacitor bank on the primary and the secondary side needs at least two capacitors in series to withstand the voltage and still have some safety margin. To be able to reach 16.38 nF, each capacitor on the primary side needs 10 capacitors in parallel which is also the case for the capacitors on the secondary side. The total capacitance for each capacitance bank is expressed as

$$C_{tot,1} = \frac{3.3\ nF \cdot 10}{2} = 16.5\ nF \tag{4.61}$$

$$C_{tot,2} = \frac{3.3\ nF \cdot 10}{2} = 16.5\ nF. \tag{4.62}$$

This means that 40 capacitors will be used in the two capacitor banks. The total capacitance was chosen to be a little bit higher than 16.38 nF, this is due to that when using compensation it is important to make sure that the circuit does not become capacitive. The circuit can become capacitive if for example the frequency is too low or the value of the capacitor bank is too low. It can also be done by designing the capacitance banks for a slightly lower frequency. However, this method was not used in this case due to that the desired frequency will always be achieved in the simulations.

With compensation, the current through the coil will now be shaped as a sinus wave. This means that only the fundamental frequency from the voltage signal will provide with active power. Therefore the ratio between the input voltage and the output voltage is not linearly dependent on D anymore. This means that the rms value for the fundamental frequency from a square wave needs to be calculated for every duty cycle. The result of this can be seen in Figure 4.5, for this case $n = 1$ for simplification. As can be seen from the figure the output rms value for the inductive case can never be equal to the input value. This means that if, for example, an output value of $0.7V_{in}$ is desired a duty cycle of 0.6 is needed.

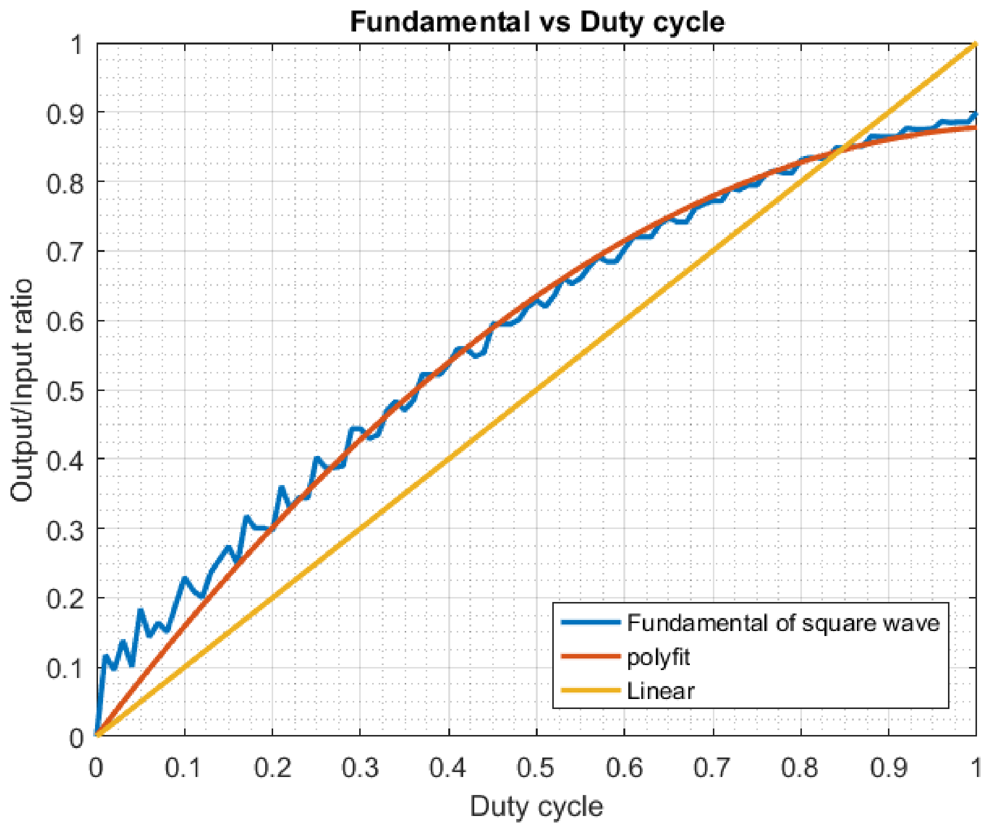

Figure 4.5: Ratio between the output and the input signal for inductive charging and conductive charging.

The values for the coils are taken from two existing coils and are set to 214 μH with $k = 0.19$. The turn ratio of the transformer is 13/8. The input voltage for the DC-step is set to 450 V. By looking at the figure it can be seen that the output signal will not increase linearly with the duty cycle for inductive charging. For example a duty cycle of 0.7 gives that the rms value for the fundamental frequency of the square wave will be 0.7719 of the input signal. This means that the voltage on the output will be

$$V_{out,1} = \frac{450\ V \cdot 0.7719}{13/8} = 214\ V \tag{4.63}$$

The equivalent series resistance for the coil is approximated from [12] where the turn ratio for the coils is 9:9 and the resistance and inductance values are $R_1 = 122.7\ m\Omega$, $R_2 = 150.8\ m\Omega$, $L_1 = 115.79\ \mu H$ and $L_2 = 132.6\ \mu H$. The turn ratio from this project is close to the turn ratio for the chosen coil in this project, however the chosen inductance is 214 μH which is almost twice as big as in [12]. Therefore it is assumed that the resistance for the chosen coils will be linear to the increase of inductance. So the resistance for the primary and secondary side can be expressed as

$$R_1^* = 122.7\ m\Omega \frac{214\ \mu H}{115.79\ \mu H} = 226.77\ m\Omega \tag{4.64}$$

$$R_2^* = 150.8\ m\Omega \frac{214\ \mu H}{132.6\ \mu H} = 243.37\ m\Omega \tag{4.65}$$

In [12] a frequency of 22 kHz was used and due to that the resistance is depending on the skin depth, δ, and the used frequency for this project is 85 kHz which means that the resistance will be even higher. The skin depth can be expressed as

$$\delta = \sqrt{\frac{2\rho}{2\pi f \mu}} \tag{4.66}$$

where ρ is the resistivity of the conductor and μ is the permeability of the conductor. The conductors are made out of copper and $\rho = 1.68 \cdot 10^{-8}\Omega m$ and $\mu = 1.256629 \cdot 10^{-6} H/m$. The resistance can be expressed as

$$R_{AC} = \frac{l}{\pi(D-\delta)\delta} \tag{4.67}$$

where l is the length of the conductor and D is the diameter of the conductor. For simplicity $D >> \delta$ which gives that (4.67) can be expressed as

$$R_{AC} = \frac{l\rho}{\pi D \delta}. \tag{4.68}$$

The ratio between the resistance in this project, R'_{AC}, and the resistance from [12] can be expressed as

$$\frac{R^*_{AC}}{R_{AC}} = \frac{\frac{L^*\rho}{\pi D^* \delta^*}}{\frac{L\rho}{\pi D \delta}}. \tag{4.69}$$

Both cases uses copper and by implementing (4.66) in (4.68) and assuming that the diameter is equal for both cases and that the length is linearly proportional to the amount of turns the resistance for the primary side can be calculated as

$$R^*_{AC} = \frac{\frac{l^*\rho}{\pi D^* \delta^*}}{\frac{l\rho}{\pi D \delta}} R_{AC}. \tag{4.70}$$

The equivalent series resistance for the primary and the secondary side when AC is taken into consideration is then expressed as

$$ESR_{1,AC} = 226.77\ m\Omega \frac{13 \cdot 85\ kHz}{9 \cdot 22\ kHz} = 1266\ m\Omega \tag{4.71}$$

$$ESR_{2,AC} = 243.37\ m\Omega \frac{8 \cdot 85\ kHz}{9 \cdot 22\ kHz} = 835.8\ m\Omega \tag{4.72}$$

It is important to state that these resistances are just approximations and may differ from the correct resistance but it shows in what range the resistance will be for this case.

The whole setup that was used in LTspice IV can be seen in Figure 4.6. As can be seen a big resistance is added between the two coils, this is due to that the secondary side needs to be connected to the primary side to complete the simulation. Also a spice directive is used to define the parameter of the transformer.

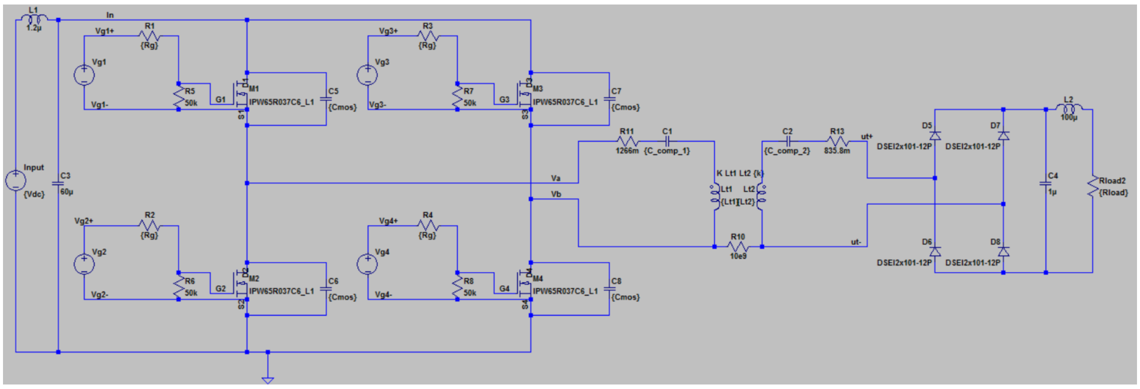

Figure 4.6: Circuit of the inductive charging setup in LTspice.

4.4 Setup for combined system

To be able to successfully combine these two different systems into a single system a well structured topology is needed but it is also important to keep the quality of the two systems so two good systems will not become one bad system. A simple way of keeping the quality of the two systems is to make everything in parallel as can be seen in Figure 4.7. With this system it is possible to perform conductive on-board charging. However this means that all power electronic from the conductive part as well as the receiver coil and the rectifier from the inductive part will be inside the EV. As mentioned before there is already a lack of space in the EV, therefore, it is probably not a good idea to add the inductive parts in an already narrow space.

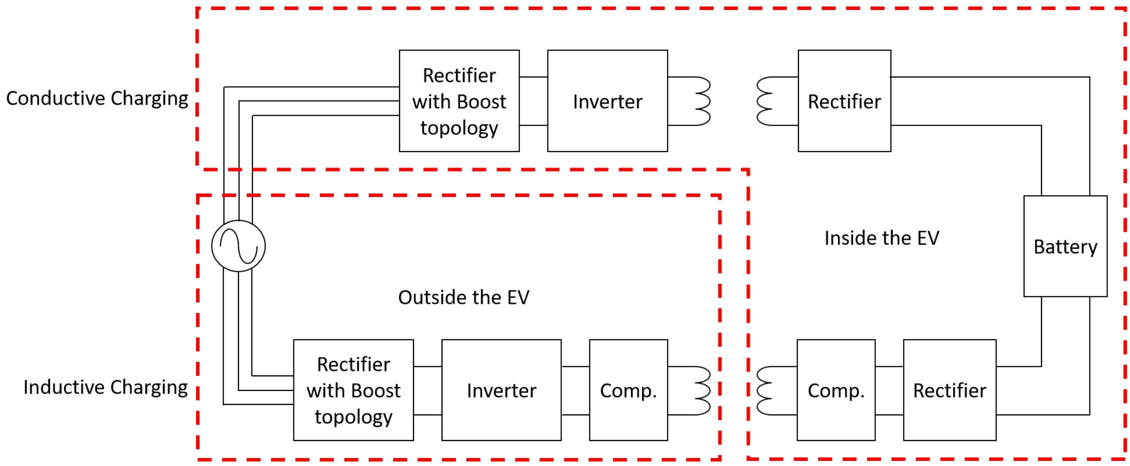

Figure 4.7: Parallel setup for the combined system with on board charging for the conductive part.

If off-board charging was used instead on the parallel setup it would set free a lot of space in the EV due to that the only thing that will be inside the EV now would be the secondary part of the inductive part. The topology for this can be seen in Figure

4.8. This means that the weight of the EV would be reduced and more space would be available for other features. However, this method can create problems for the driver. For example, one problem may be that the driver can now only charge the EV at places where this power electronic is available. It can also be seen that there are some duplicates of some components in the parallel system. One of the tasks that was mentioned in the introduction was to reduce the amount of components so this combined system would be smaller than two separate systems.

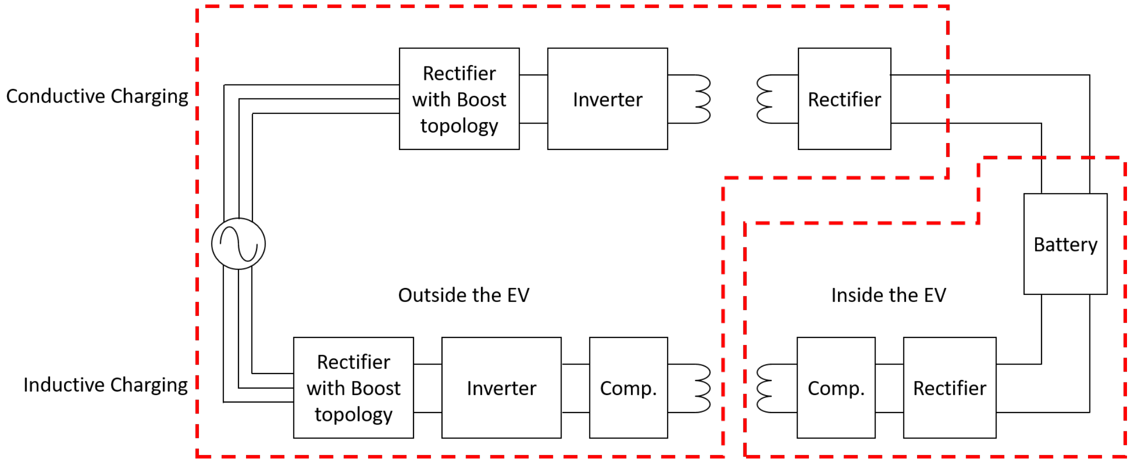

Figure 4.8: Parallel setup for the combined system with off board charging for the conductive part.

One solution to reduce the amount of components can be to use the topology that can be seen in Figure 4.9. From the figure it can be seen that the conductive and the inductive system uses the same rectifier and inverter. The rectifier connected to the battery can consist of exactly the same components but it is not possible to only use one rectifier due to that the one that belongs to the conductive charging system is not inside the car as the rectifier which belongs to the secondary side of the inductive charging system.

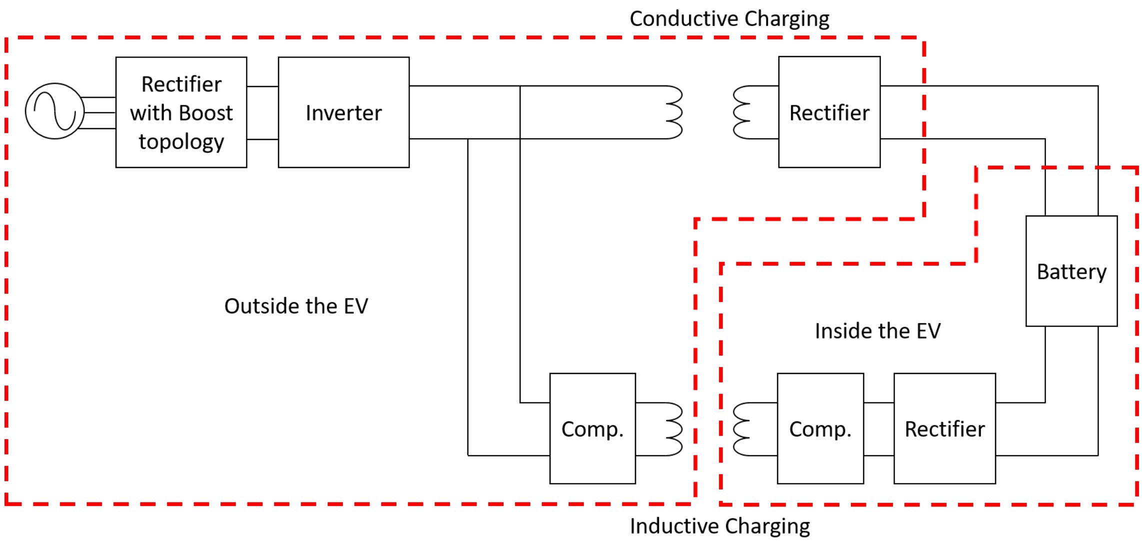

Figure 4.9: Parallel setup for the combined system

The rectifier is a passive component and the only thing that needs to be checked is to make sure that the diodes can withstand the voltage and the current levels. However, for the boost converter the inductor has to be specified so it satisfies both systems requirements. This is due to that the inductor is a passive component which is not the case for MOSFET of the boost converter, which decides the duty cycle. The duty cycle can be specified to be a certain value but it can also be specified to be two different values which is depending on which type of charging method that is used. This means that the boost converter needs to know what type of charging method that is going to charge the car and therefore it will be re-programed every time the charging system is connected to the EV. The inverter also needs to be a compromise to be able to handle both systems. Due to that the DC voltage on the inverter is 600 V for Case 2 and the chosen MOSFETs can withstand 700 V this topology is not optimal for the combined system. This is mainly due to that it is desirable to have a margin of around 50 % and for this case, the margin is only 100 V.

The phase shift controller and ZVS will be used for this inverter as well as in the previous setups to reduce the switching losses. When it come to the transformer it is quite obvious that there has to be two of them, one for the conductive part and one for the inductive part. As mentioned before the whole transformer for the conductive setup is placed outside the car as well as the primary side of the transformer for the inductive part. The secondary side of the transformer for the inductive part is placed inside the car. Due to that one secondary side is outside the EV and one is inside the EV it is not possible to only use one rectifier. If the same rectifier would be used it would have to be placed inside the EV and then the car could have been charged with a high frequency current during conductive charging. Therefore two rectifier must be used before the power is transferred to the battery.

5
Results

This chapter will present simulation results for the different components that has been designed. The results will be explained and discussed in this chapter and at the end a cost analysis of the designed systems will be presented.

5.1 Simulation results for the Boost Converters

Figure 5.1 shows the efficiency for the two different boost converters and as can be seen the efficiency is almost 100 % for $D < 0.7$. As mentioned earlier the parasitic components have a huge impact on the transferred power at higher duty cycles which explains the drop in efficiency between $D = 0.6$ and $D = 0.7$. The Duty cycle was stepped with 0.1 but due to that the dip appeared between 0.6 and 0.7 and one of the converters was designed with a duty cycle of 0.617 an extra simulation at 0.65 was made. The load was set so the output power always was 3.3 kW in this simulation.

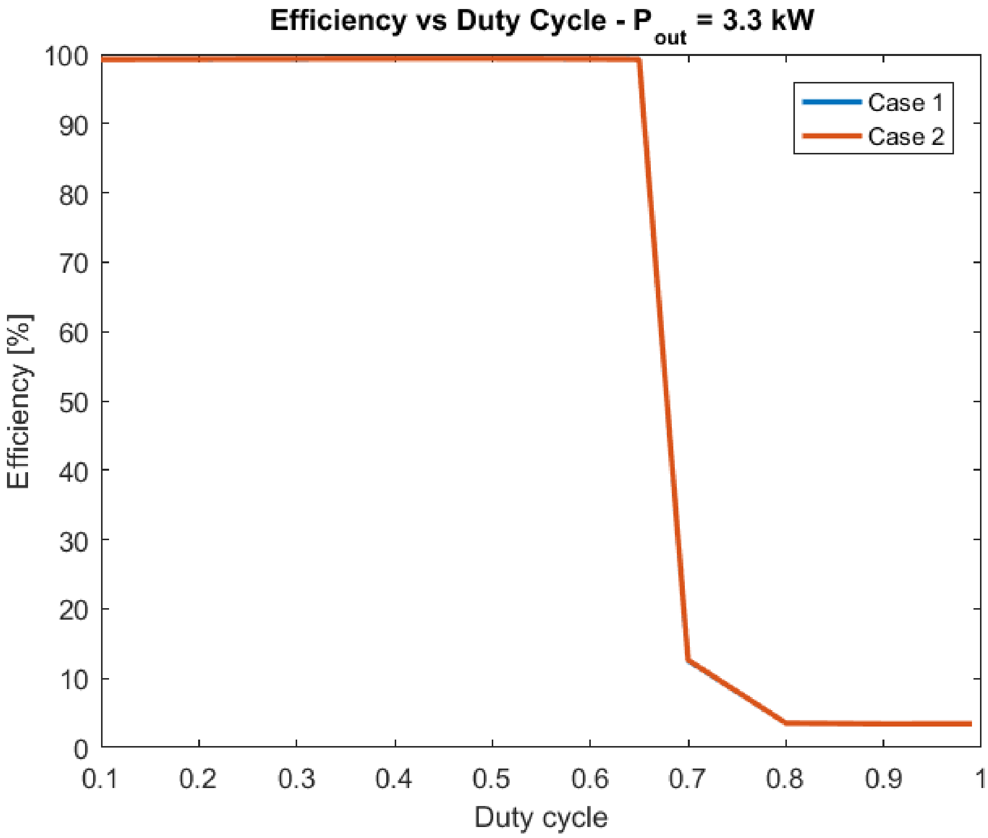

Figure 5.1: Efficiency curve for different duty cycles.

However, it is impossible to see any difference for the two different designs. By zooming in on the plot it is possible to observe the efficiency more detailed. The zoom in of Figure 5.1 can be seen in Figure 5.2. By only presenting the values for a duty cycle up to 0.65 it is possible to see that the efficiency is over 99 % for $D < 0.65$.

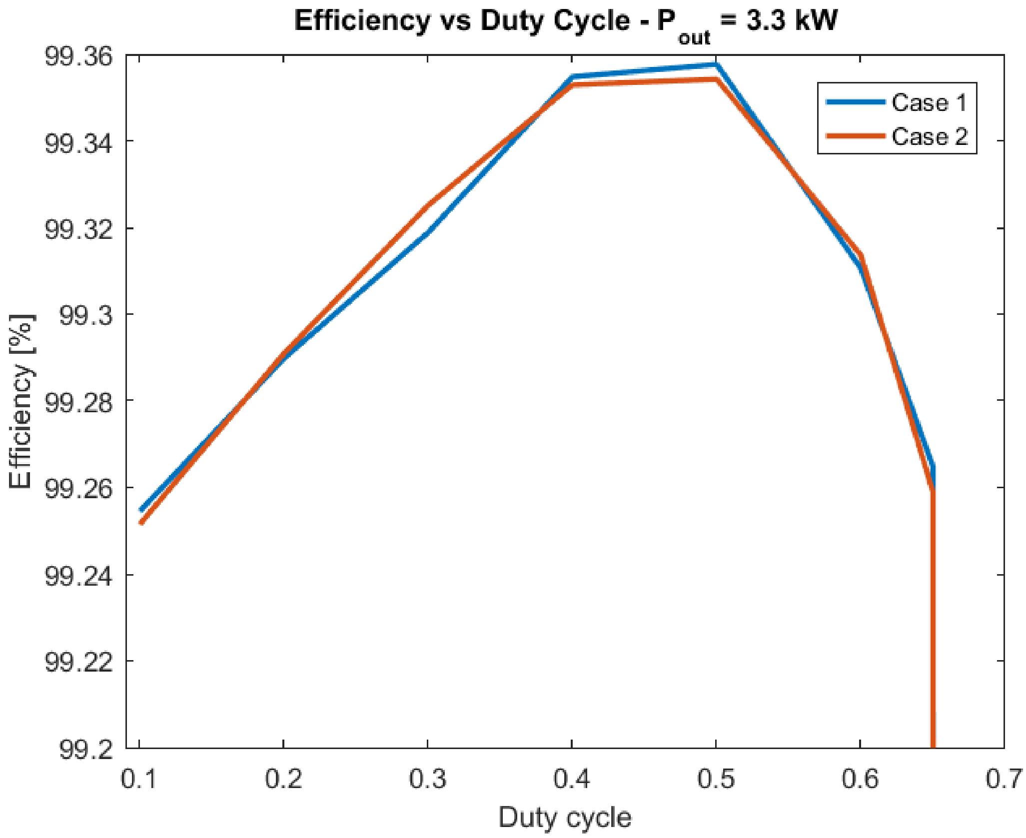

Figure 5.2: Zoomed in version of efficiency curve for different duty cycles.

To be able to see if the desired voltage level is reached, the output voltage was plotted against the duty cycle, which can be seen in Figure 5.3. From the figure it can be seen that for $D = 0.489$ a output voltage of around 450 V was achieved and for $D = 0.617$ a output voltage of around 600 V was achieved. It is also possible to see the impact of the parasitic components which causes the output voltage to flatten out for $D > 0.7$.

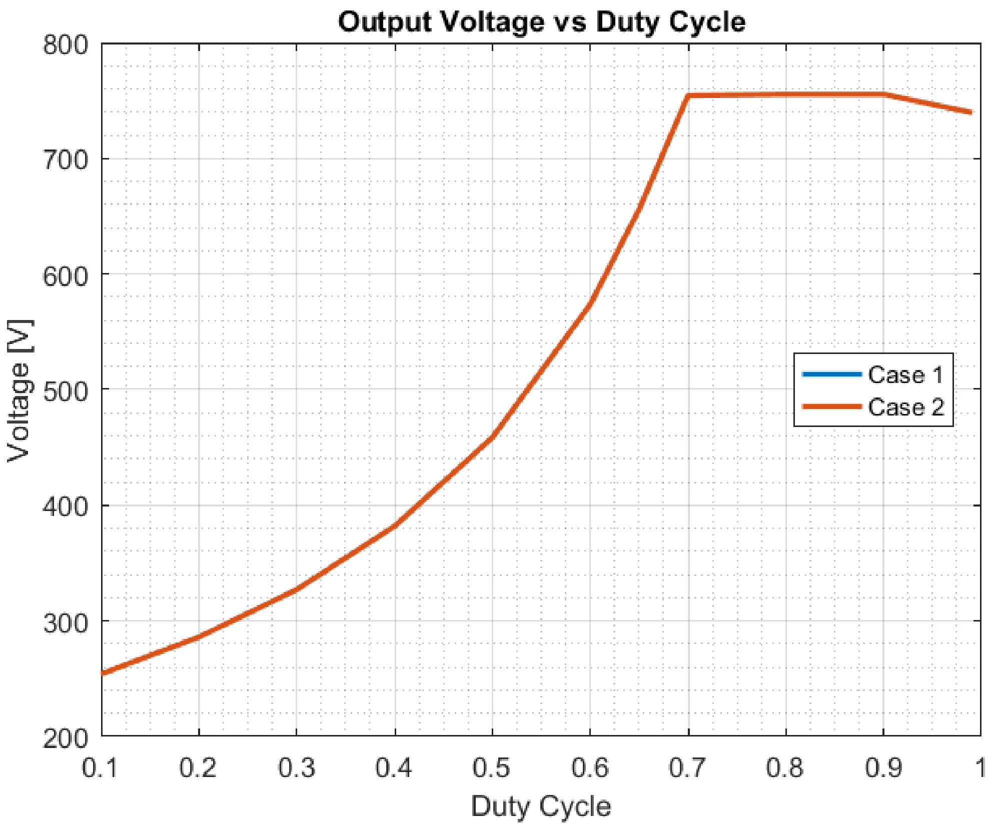

Figure 5.3: Output voltage for the two boost converters for different duty cycles.

The voltage ripple must also be investigated due to that it is desired to have a ripple as close to zero as possible. The output voltage for the two boost converters can be seen in Figure 5.4. As can be seen the peak to peak voltage is approximate 1 V which is good, however it was desired to have an even lower voltage ripple.

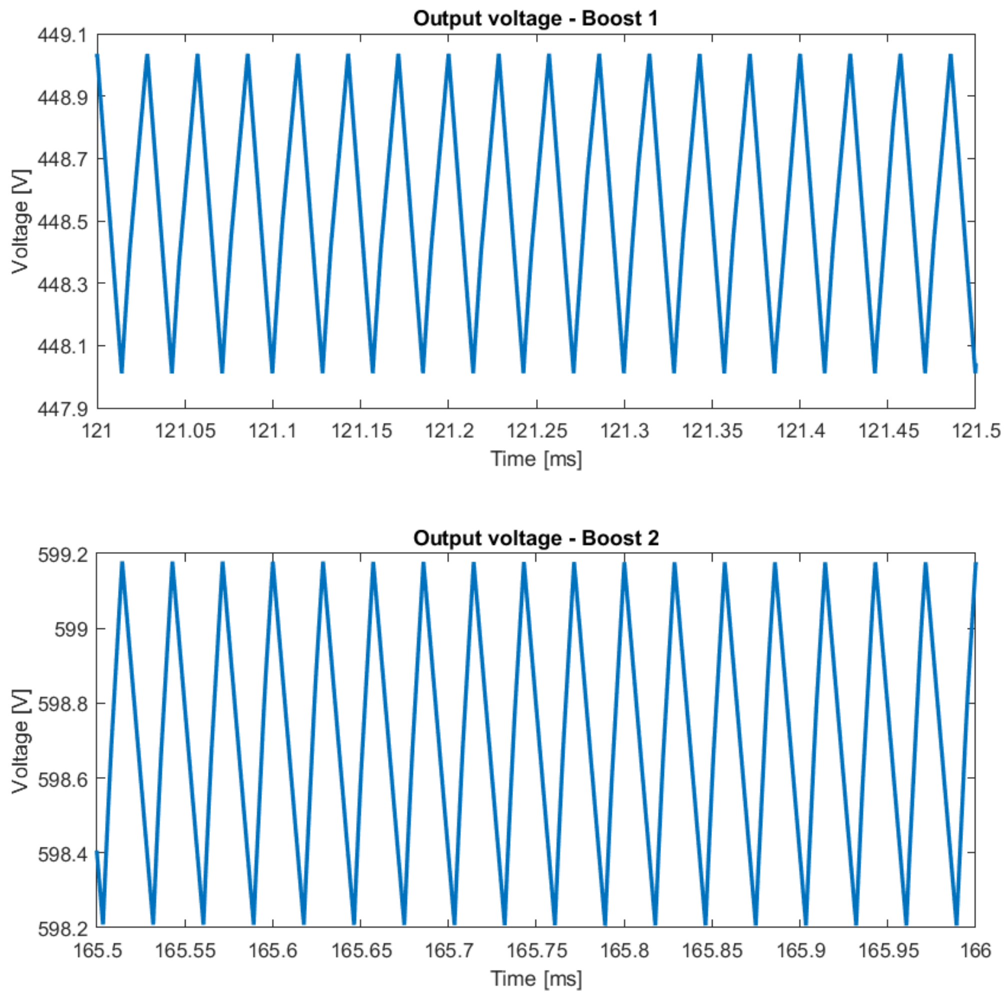

Figure 5.4: Output voltage from the two boost converter with ripple.

The boost converters was also tested for different power levels with the nominal duty cycle. In Figure 5.5 it can be seen that the efficiency was over 99 % for all power levels between $1 - 7\ kW$. It can also be seen that the boost converter with a lower duty cycle has a slightly higher efficiency. With these simulations it can be stated that the desired DC voltage for the DC/DC setups was achieved for both of the boost converter with almost no losses.

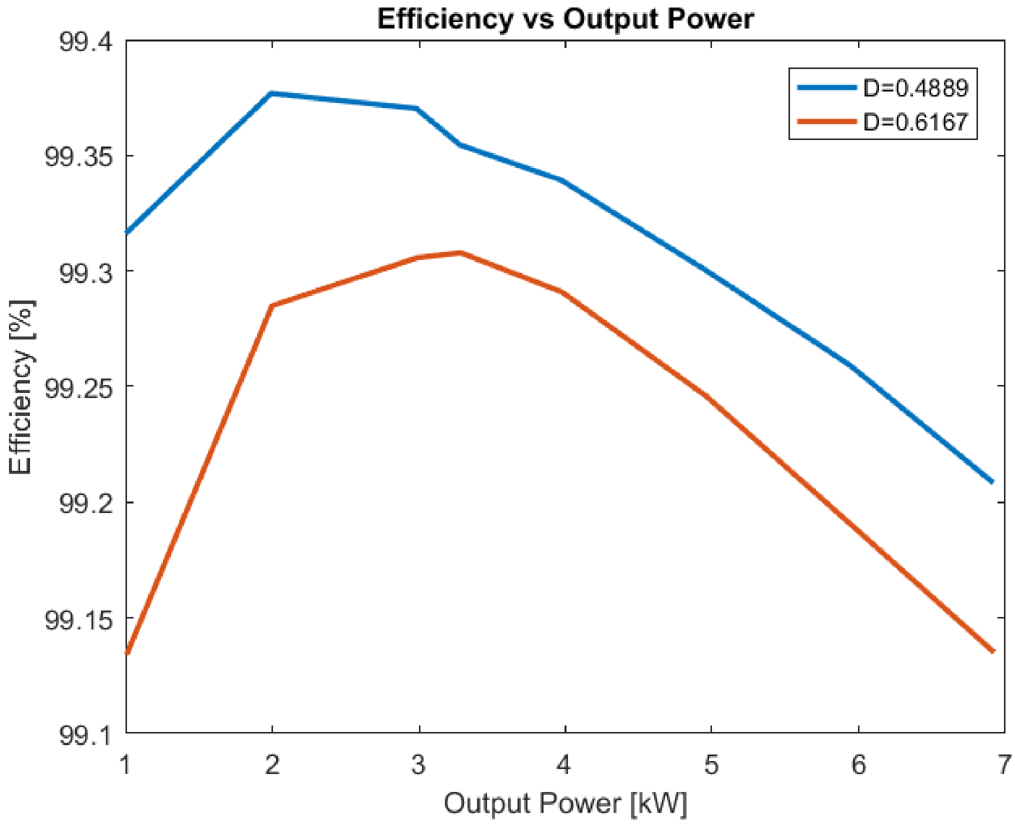

Figure 5.5: Zoomed in version of efficiency curve for different duty cycles.

5.2 Simulation results for the DC/DC steps

The DC/DC step was simulated by applying a pure DC voltage on the input of the DC/DC step which is the same as assuming that the boost converter can supply a pure DC signal to the DC/DC step. With this assumption the simulation time for the DC/DC step can be reduced heavily due to that the frequency of the grid is 50 Hz while the frequency for the DC/DC step is 85 kHz. This means that the only time period that will be taken into consideration will be the one for the DC/DC step which is around 11.76 μs, compared to the time period for the grid which is 20 ms. This assumption is assumed to have an extremely little impact on the results for the whole system due to that the boost converter provided with the desired voltage level with an extremely small voltage ripple. The three conductive cases were designed to have an output voltage of 100 V, 450 V and 600 V and the output current for these cases should then be 33 A, 7.33 A and 5.5 A to be able to deliver 3.3 kW. During the simulations it was noticed that the output voltage for Case 1 was far too low and it was not possible to supply 3.3 kW for this system. Therefore the input voltage for the DC/DC step was set to 550 V instead of 450 V to be able to supply the load with 3.3 kW. The output voltage and the output current for all three cases can be seen in Figure 5.6.

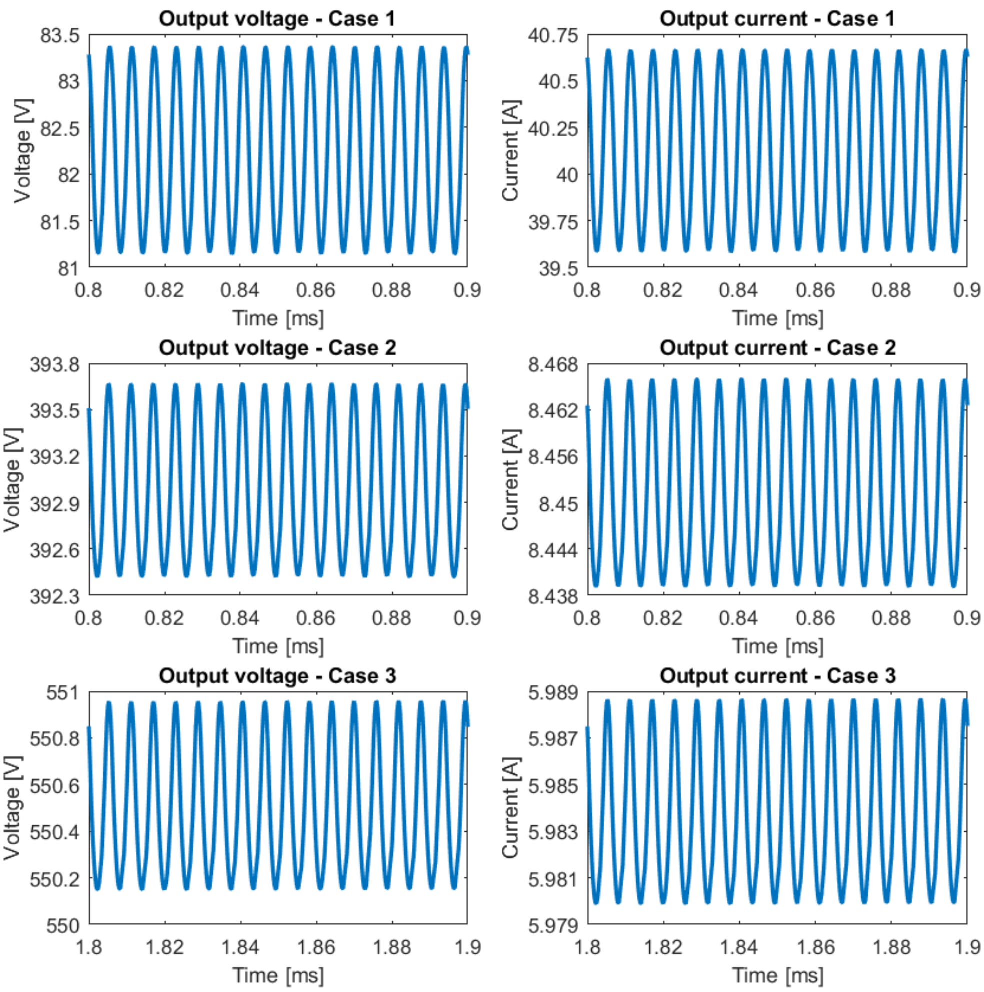

Figure 5.6: Output signal for the three conductive cases.

As can be seen the voltage level is lower than it was designed for and is believed to be caused due to the leakage inductance in the transformer. The voltage could be increased by increasing the number of turns on the secondary side but due to that the system could supply the desired power level, 3.3 kW, this was not needed. The peak to peak voltage for Case 1, 2 and 3 was 2.2 V, 1.24 V and 0.8 V, respectively while the peak to peak current was 1.07 A, 26.7 mA and 5.98 mA. The systems were designed to have a voltage ripple of 1 V, and as can be seen Case 2 and 3 is close to 1 V while Case 1 is 2.2 V. The deviation for Case 1 is most likely related to that the input voltage for Case 1 was increased. The output capacitance for Case 1 was calculated with (4.56) which is depending on (4.15) and (4.20). By increasing the input voltage, D_1 from (4.15) will decrease. By decreasing D_1, $\Delta I_{0,1}$ that is calculated in (4.20) will increase which leads to that the capacitance that is calculated from (4.56) is not big enough.

To be able to confirm if the lower voltage is caused due to the leakage inductance of the transformer the voltage and the current through the transformer must be investigated. To be able to do this the input voltage, the input current, the output voltage and the output current was plotted for three different scenarios. It was chosen to do these simulations for Case 2 due to that this case was designed with the biggest leakage inductance. However, Case 1 could also have been investigated due to that the voltage deviated in comparison to the designed voltage for this case. The first scenario was the designed case, which means that $L_{\sigma,1} = 15\ \mu H$ and $L_{\sigma,2} = 3\ \mu H$. For the second scenario $L_{\sigma,1}$ was kept as usual and $L_{\sigma,2} = 0\ \mu H$. This means that the secondary coil has no leakage inductance. In the third and final scenario, $L_{\sigma,1} = 1\ \mu H$ and $L_{\sigma,2} = 0\ \mu H$ which means that the secondary coil has no leakage inductance while the primary coil has a small leakage inductance. It was chosen to not set $L_{\sigma,1} = 0\ \mu H$ due to that it was desired to still have ZVS during the simulations. The results for the three scenarios can be seen in Figure 5.7-5.9, respectively. For the first scenario it can be seen that the current rises quite slow when a positive voltage is occurred which can be explained with the relation between the voltage and the current for an inductor which is written as

$$V_L = L\frac{di_L}{dt}. \tag{5.1}$$

This means that if L is increased and the voltage is kept the same the change in current will decrease. By looking at lower plot it can be seen that on the secondary side the current has the same shape as for the primary side. However, the width of the voltage curve is a bit smaller in comparison to the primary side which means that the RMS value of the output voltage of the transformer will be smaller than expected.

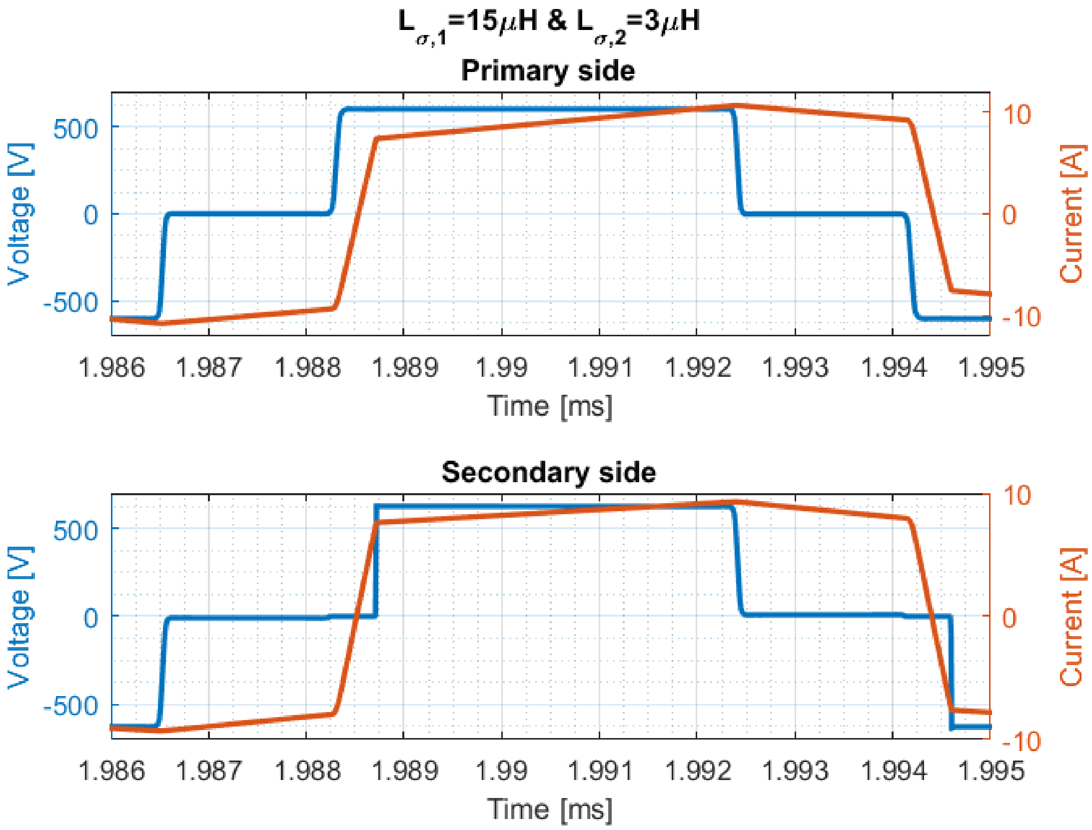

Figure 5.7: Voltage and current characteristics for the primary and the secondary side of the transformer. Simulation values are taken from Case 2.

By removing the leakage inductance on the secondary side, the steepness of the current is changed but the change is so small that it can barely be seen. The width of the voltage curve is still smaller than the voltage curve on the primary side which gives that the RMS value of the output voltage for the transformer is still smaller than expected. Due to that the changes for this scenario was negligible compared to the previous scenario it concluded that the leakage inductance on the secondary side has almost no impact on the output voltage.

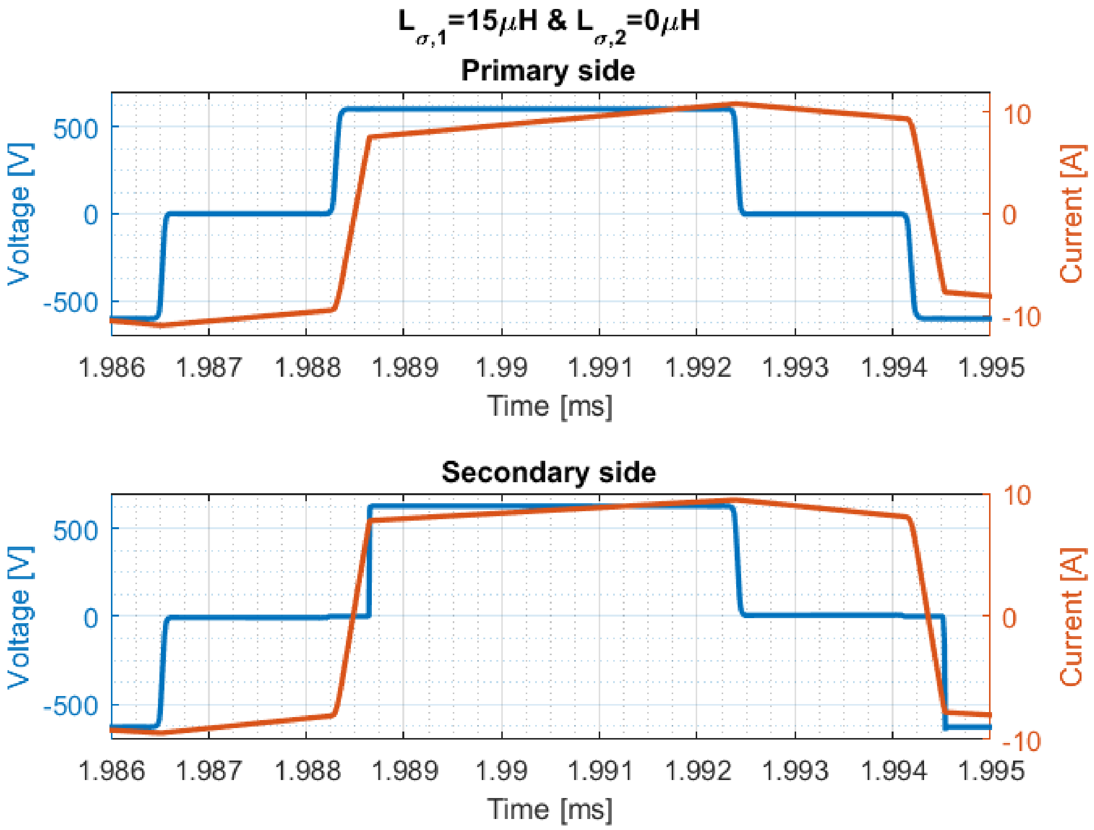

Figure 5.8: Voltage and current characteristics for the primary and the secondary side of the transformer. Simulation values are taken from Case 2 but the leakage inductance on the secondary side is removed.

In the last scenario it can be seen that the width of the voltage curve for the secondary side is equal to the one on the primary side. This means that the desired voltage level will be received for this scenario. However, this concludes that the added leakage inductance which is used to achieve ZVS will lower the output voltage a bit.

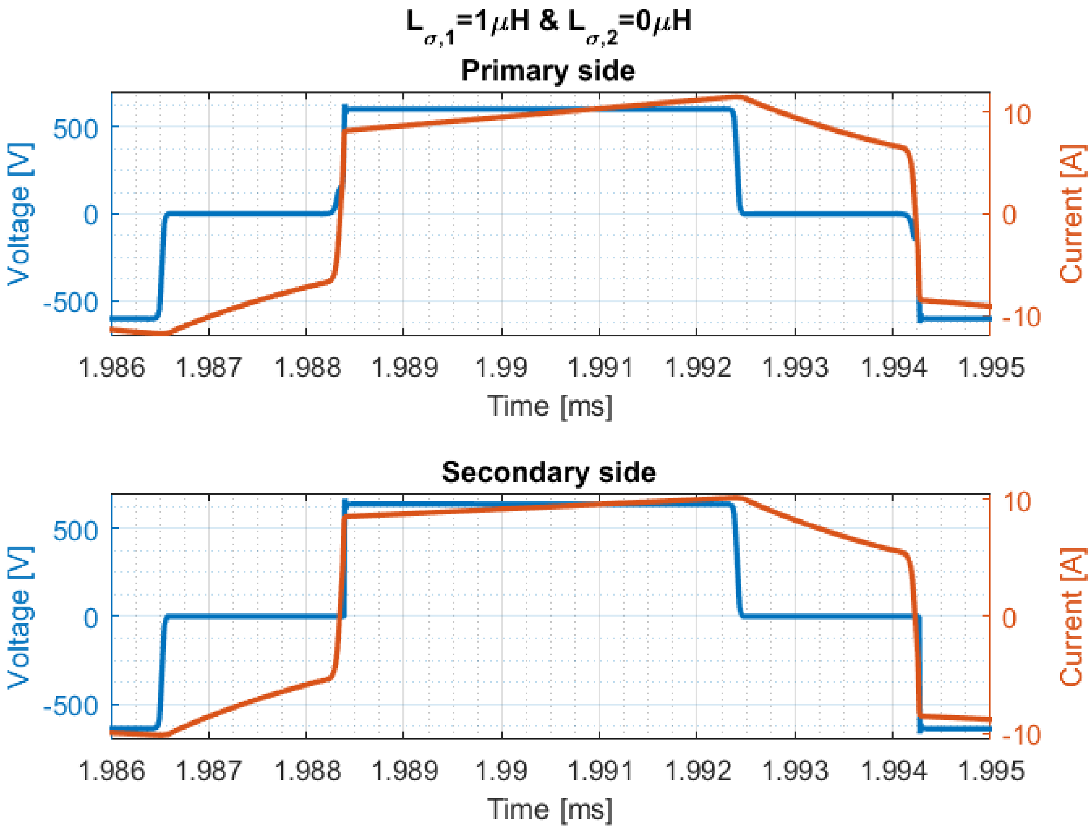

Figure 5.9: Voltage and current characteristics for the primary and the secondary side of the transformer. Simulation values are taken from Case 2 but the leakage inductance on the secondary side is removed and $L_{\sigma,1} = 1\ \mu H$.

To see if the calculated output ripple is correct, the current through the inductor L_f must be inspected. The current ripple can be seen in Figure 5.10. L_f was set so that the output current ripple should be 10 % of the nominal output current. However, as can be seen, the output current is higher than the nominal current which is due to that the desired output voltage was not achieved. ΔI_0 is the difference between the peak of the current and the average value of the current. The peak for all three cases are 44.6 A, 9.29 A and 6.53 A which gives that ΔI_0 is approximately 10 % for all three cases.

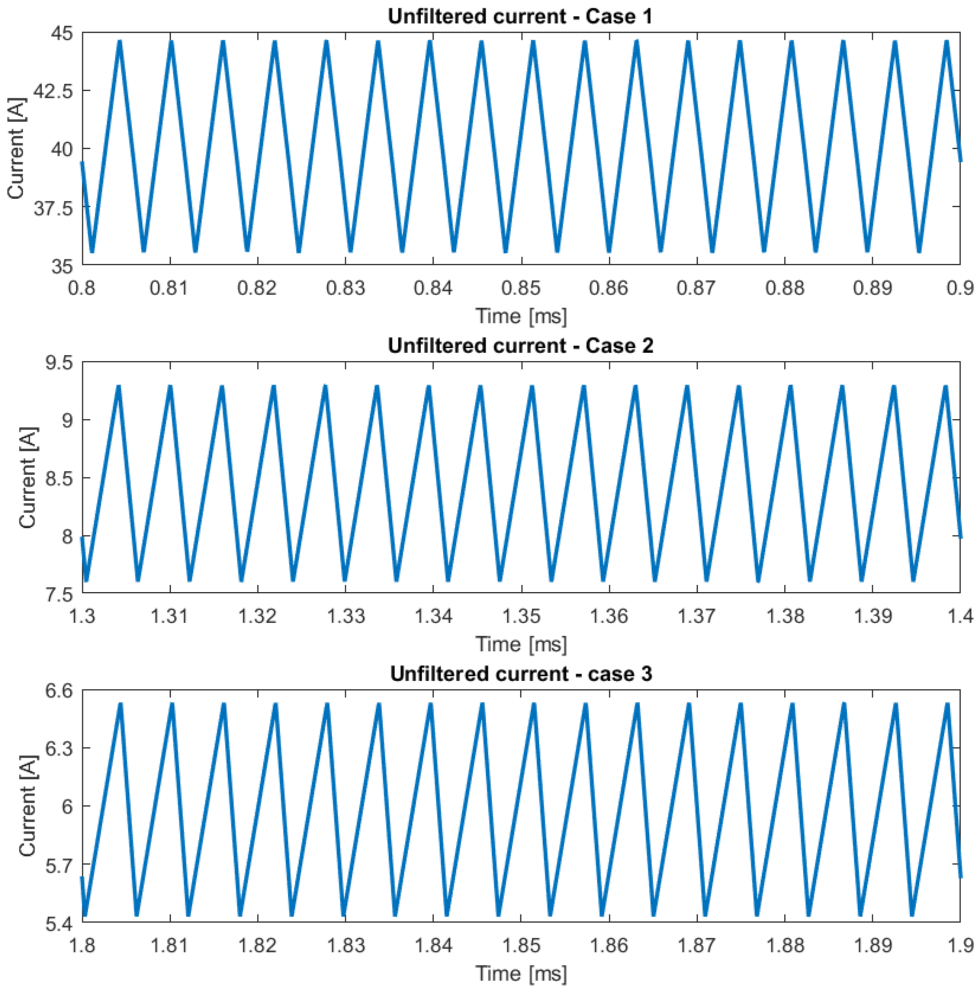

Figure 5.10: Output current with ripple.

As mentioned before, to increase the amount of transferred active power a compensation was needed for the inductive charger. In the top plot of Figure 5.11 it can be seen that the input current to the transformer is lagging the input voltage of the transformer. Due to that the phase shift is around 90° almost no active power is transferred in this case. However, as can be seen in the bottom plot, by adding the two capacitors that was calculated earlier the phase shift between the current and the voltage is removed. The result of this is that more active power will be transferred without increasing the input power.

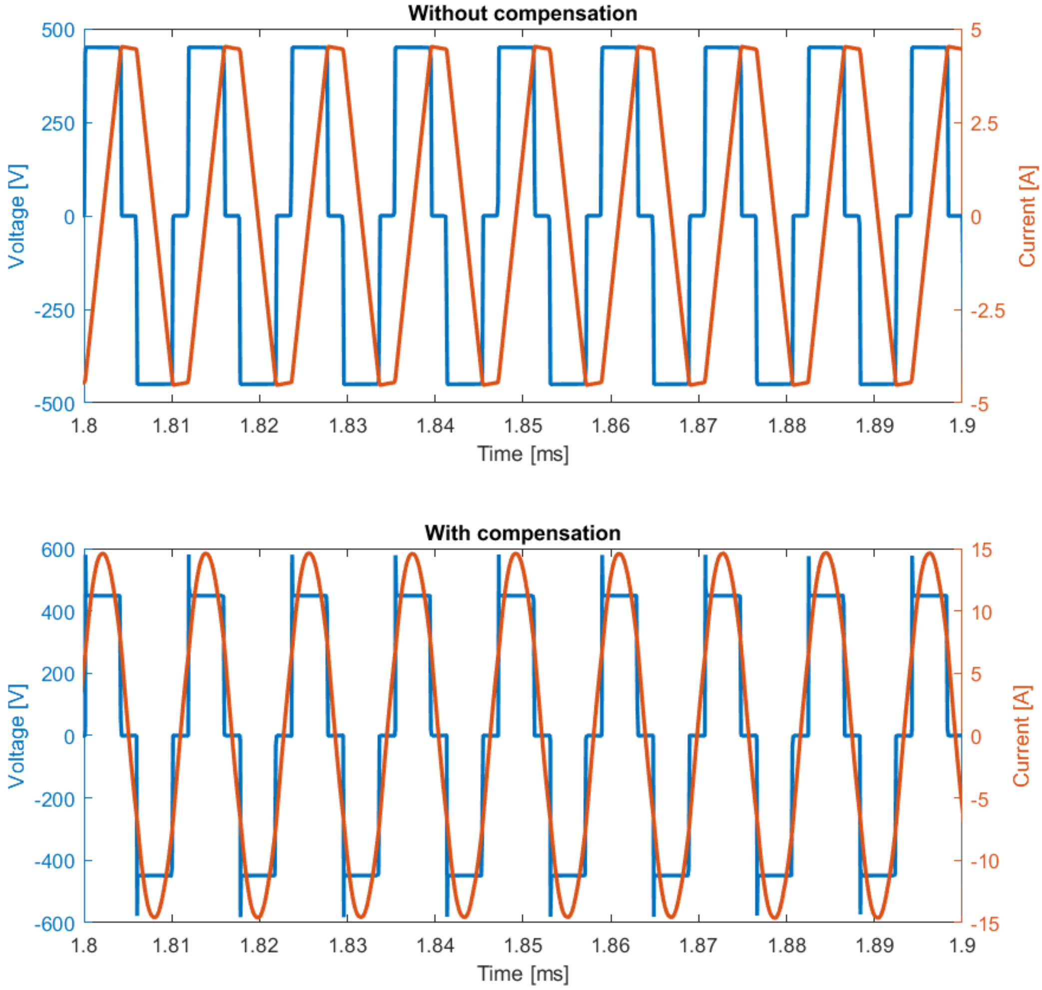

Figure 5.11: Input voltage and input current without and with series compensation.

It was stated earlier that the only frequency that will contribute with active power is the fundamental frequency of the square wave, this is due to that the current through the transformer is sinusoidal, as was showed in the bottom plot of Figure 5.11. The ratio between the output voltage and the input voltage for the wireless system can be seen in Figure 5.12. As can be seen, the shape of the simulated ratio is close to the calculated fundamental ratio of the square wave. It can be seen that the biggest deviations occur for low duty cycles, this is believed to be caused due to that ZVS is not achieved.

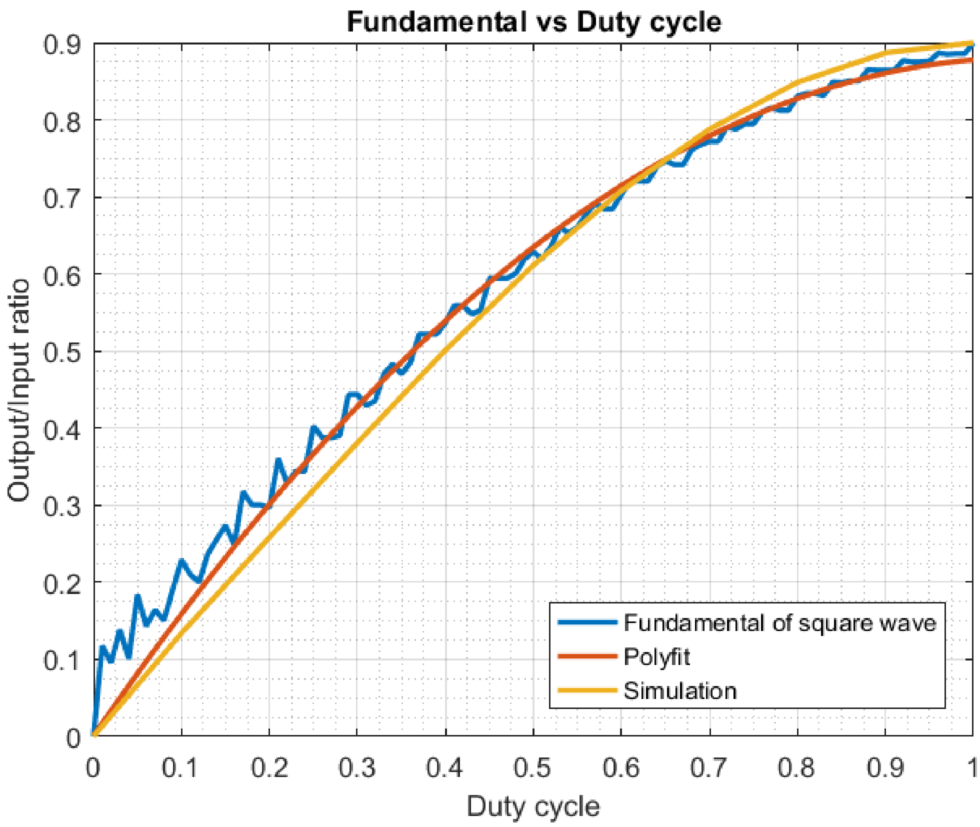

Figure 5.12: Calculations and simulations for the ratio between the output and the input signal for inductive charging.

By changing the duty cycle of the inverter different power levels will be acquired. The output power for the DC/DC step for both the conductive and the inductive cases can be seen in Figure 5.13. From the figure it can be seen that the power level is smoothed out a bit for higher duty cycles for the inductive case while it keeps increasing for the conductive cases.

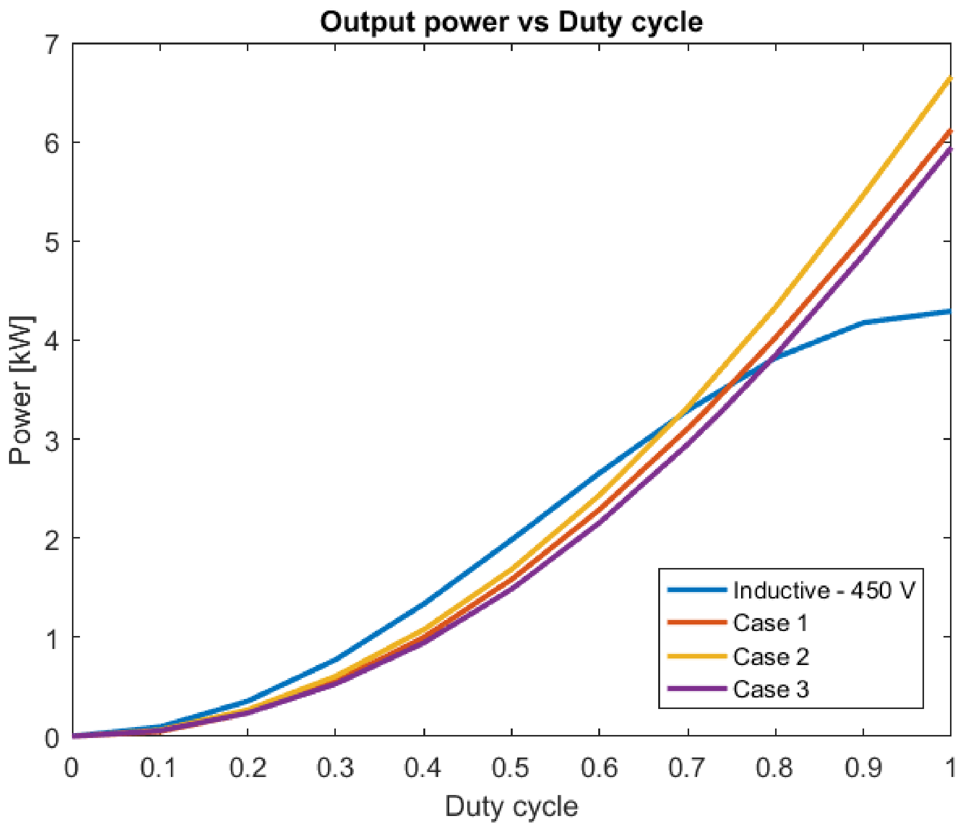

Figure 5.13: Output power from the DC/DC step.

The efficiency of the DC/DC step can be seen in Figure 5.14. As can be seen the efficiency increases with the Duty cycle and then stabilises for both the inductive and the conductive cases. The reason for the low efficiency for low D is due to that the switching losses in the inverter are high for low duty cycles. By increasing the duty cycle the current will increase and ZVS will occur and the losses in the inverter will be decreased heavily. It can also be seen that the inductive charger has a lower efficiency compared to the three conductive chargers. This is mainly due to that the resistance in the transformer is higher for the inductive cases than for the conductive cases. For the inductive charger an efficiency of 85.98 % was achieved when the duty cycle was set to 0.7. However, when increasing the duty cycle to 0.9 an efficiency of 88 % is achieved. As can be seen Case 2 and Case 3 have the highest efficiency, where Case 3 is slightly higher than Case 2. For the nominal duty cycle, the efficiency is 98.42 % for Case 3 and for Case 2 the efficiency is 98.06 %. For Case 1 the efficiency at the nominal duty cycle is 92.84 %. The reason for why Case 1 have the lowest efficiency of the three conductive cases is probably due to that this case have a larger current which will increase the conduction losses for the inverter, the transformer and the rectifier.

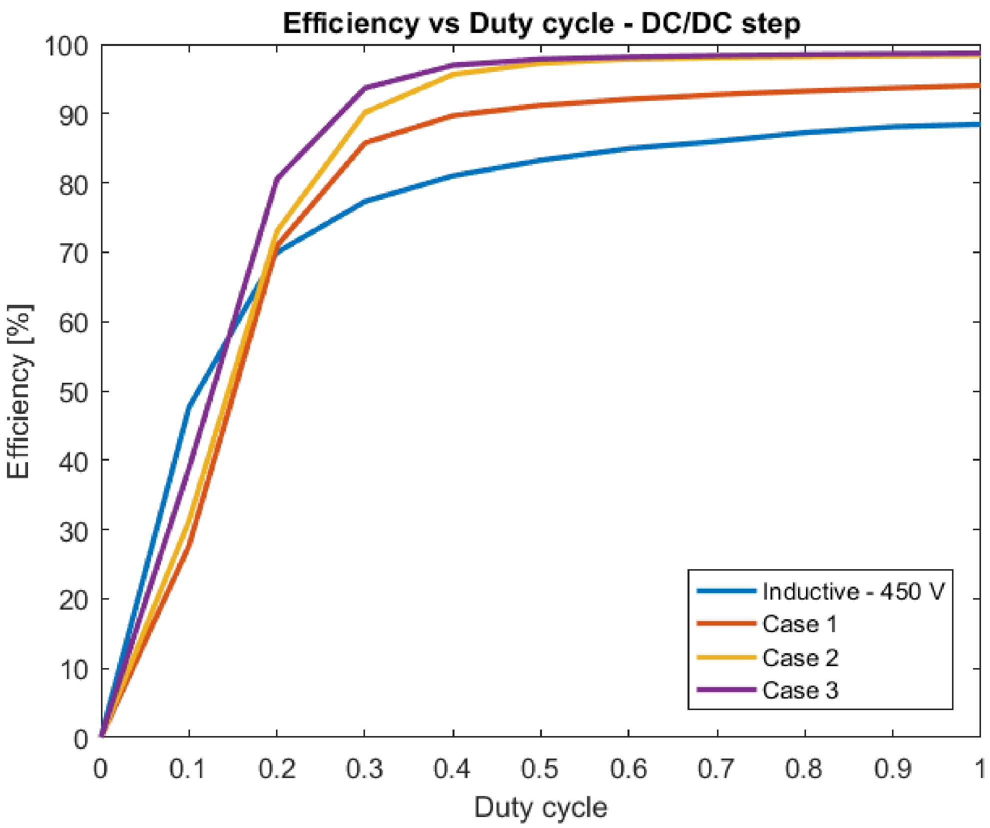

Figure 5.14: Efficiency for the DC/DC step for different duty cycles.

The DC/DC step was also tested for different power levels for the nominal duty cycle. Due to that the inductive case was not designed from scratch D was set to 0.7 for the inductive cases. The results from the simulations can be seen in Figure 5.15. It can be seen that the efficiency is lower for low power level and that the efficiency stabilises when the output power is increased. However, it can clearly be seen that the characteristics for case 1 differs a lot from the other cases. This is believed to mainly depend on that the output voltage for the three cases was somewhere below the specified voltage during the simulations, as was showed earlier. The reduced voltage on the output was mainly caused due to the leakage inductance that was added to receive ZVS and due to that Case 1 was designed for low voltage and high current the voltage drop in the system become too big. This could have been solved by increasing the amount of turns on the secondary side but due to that the two other conductive systems worked fine this modification was never made. From the figure it can be seen that Case 3 has the highest efficiency followed up by Case 2. Case 1 could not provide with more than 4 kW in the simulation due to that the voltage decreased heavily when the desired output power was increased. It can also be seen that the efficiency for the inductive case has efficiency of 85 % when the output power is between $3 - 7\ kW$.

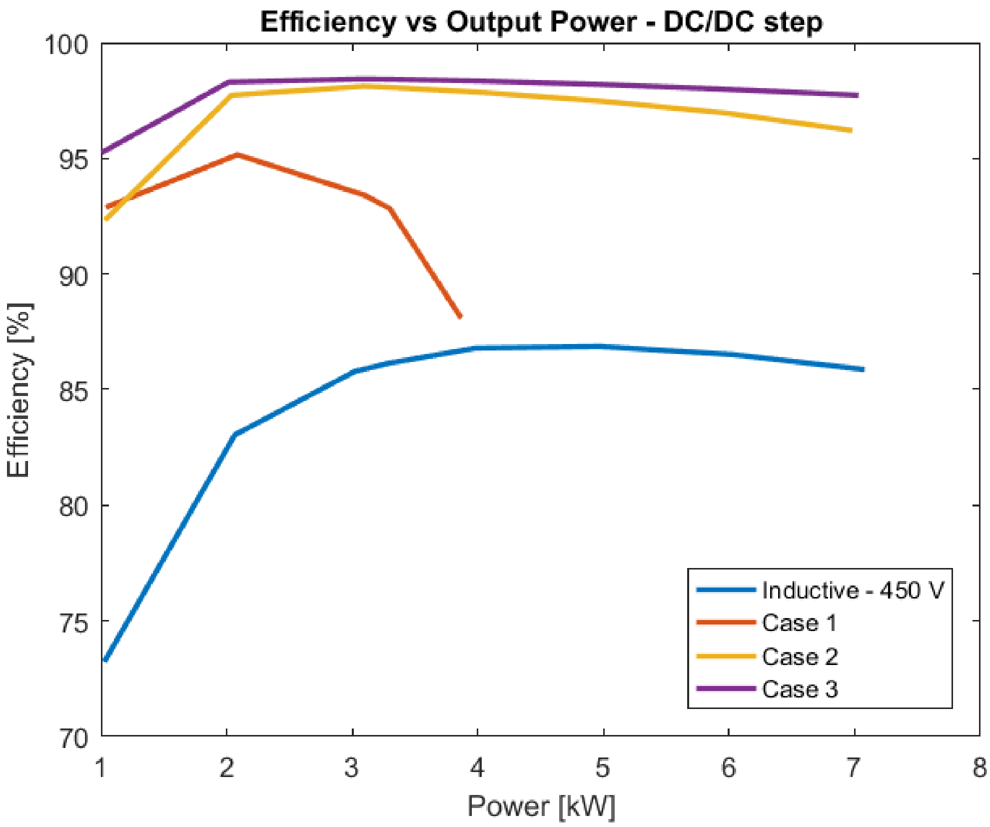

Figure 5.15: Efficiency for different output power with the nominal duty cycle.

As have been mentioned, the main reason for why the efficiency is lower for the inductive case than for the conductive case is because of the resistance of the transformer, which can be seen in Figure 5.16. The figure shows the loss distribution for the inductive and the conductive cases and as can be seen the losses in the transformer contribute with 66 % of the total losses for the inductive system. By comparing this with the losses for the conductive cases, it can be seen that for the conductive cases the rectifier contributes with the highest losses in all three cases. The contribution of losses from the transformer will increase for higher currents leaving that the contribution of losses provide from the inverter will be much smaller compared to the losses from the rectifier.

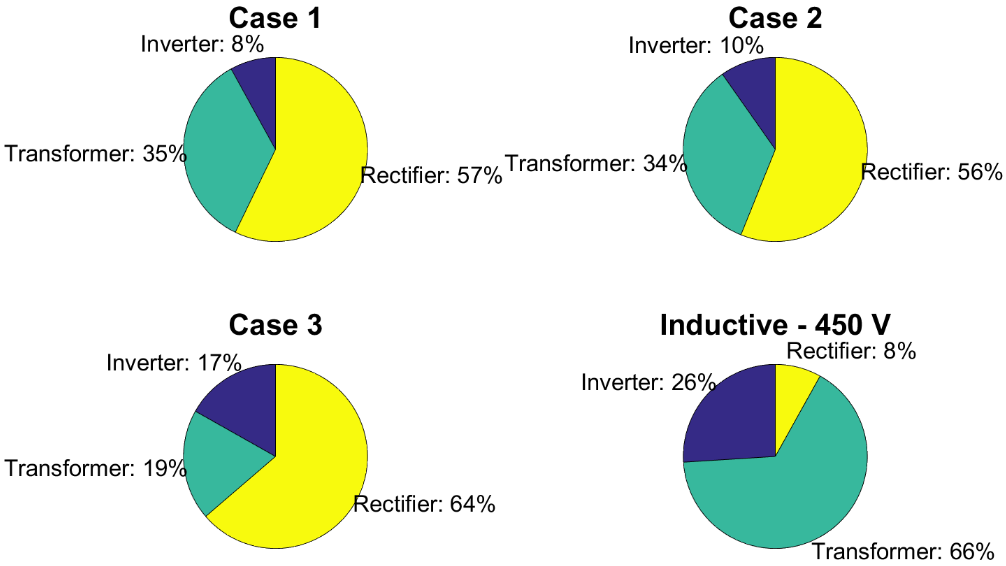

Figure 5.16: Loss distribution for the inductive and the conductive cases.

The model that was designed for inductive charging was compared with measurements from an already built inductive charger. It is important to state these two systems are not based on the same design. However the measurements shows how good performance a wireless system can achieve. The comparison between the simulations and the measurements can be seen in Figure 5.17 and 5.18. As can be seen the output power is increasing similar in the measurements compared to the simulations. However, during the measurements the output power only reached 3.3 kW but the characteristics looks the same. From Figure 5.18 it can be seen that an efficiency of 93 % was achieved during the measurements which is higher than for the simulated model. One explanation for this can be that the transformer for the real setup was made out of litz wire which is less affected by the frequency.

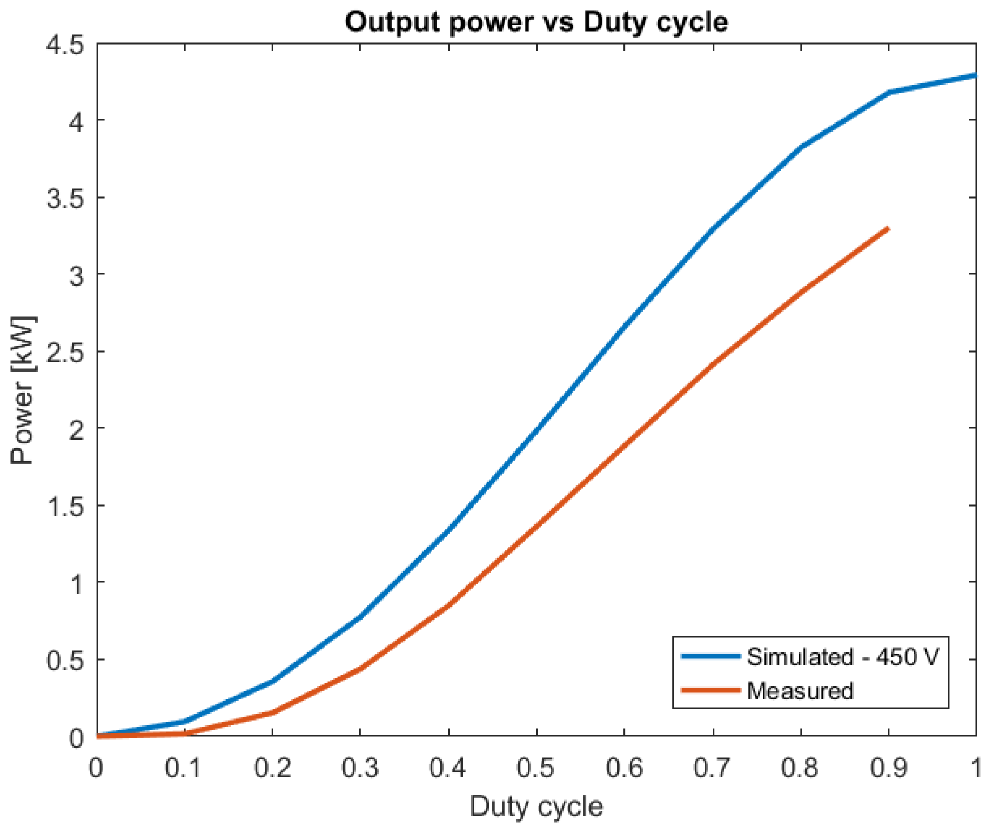

Figure 5.17: Output power for both measurement and simulations for inductive charging.

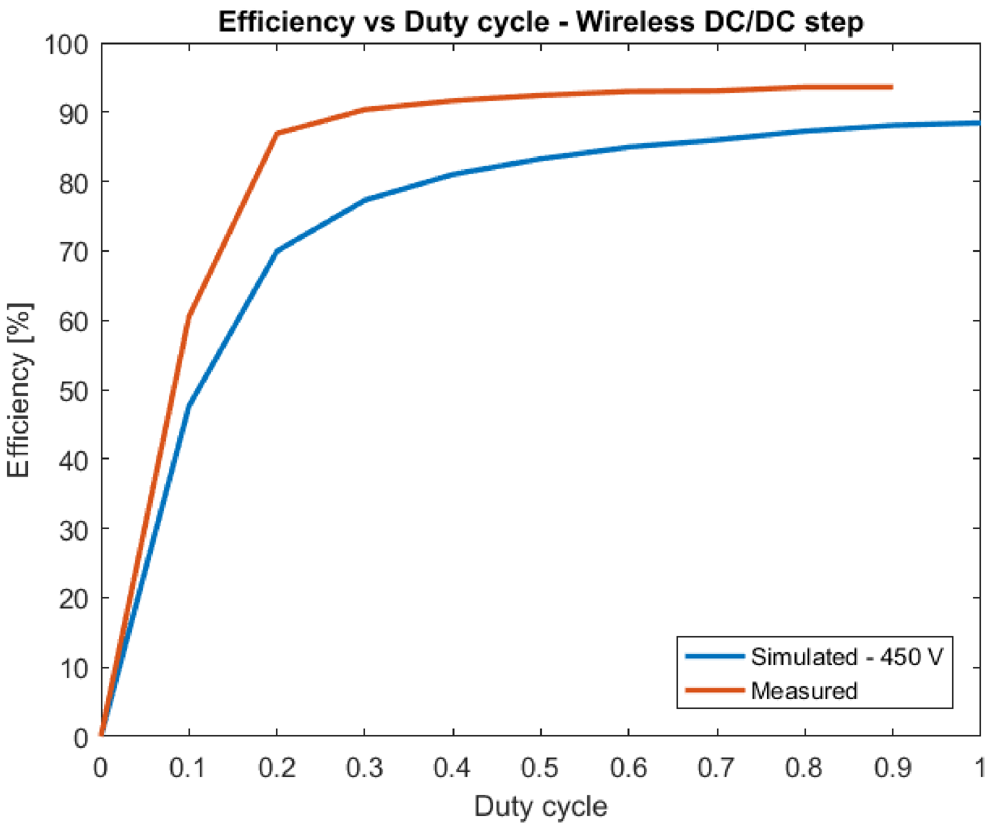

Figure 5.18: Efficiency for both measurement and simulations for inductive charging.

Due to the difference between the measured and simulated results it was decided to simulate the model without a frequency dependence for the resistances. The simulations were also made with a series compensation of 16.38 nF and 16.5 nF to be able to see if there is any difference in efficiency between the model with the calculated capacitance and the capacitor bank that was used for the cost analysis. As can be seen in Figure 5.19 the difference in efficiency when using a compensation of 16.38 nF and 16.5 nF is negligible. However, as was shown before, the increase of the resistance of the coils has a big impact on the efficiency. Without the frequency dependence an efficiency of 92.53 % was achieved when $D = 0.7$.

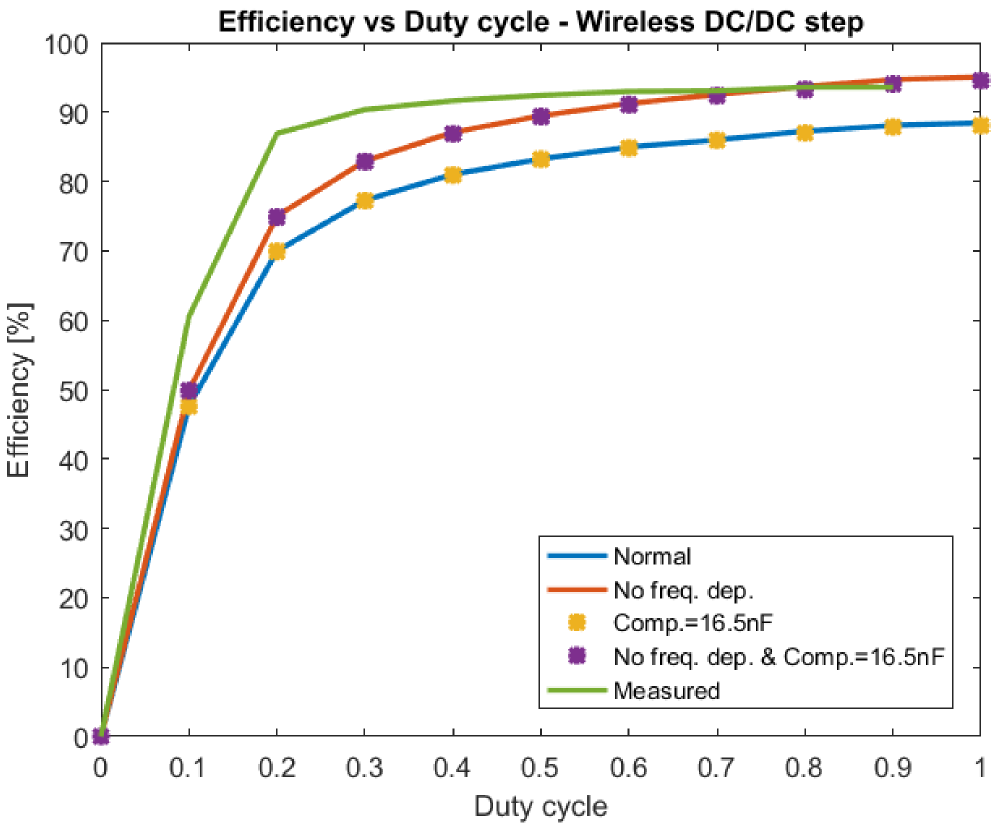

Figure 5.19: Efficiency for both measurement and simulations for inductive charging. The simulations are made with and without frequency dependence and with series compensation with both 16.38 nF and 16.5 nF.

Without the frequency dependence of the resistance in the coils, the losses in the transformer will decrease and therefore the loss contribution from the transformer will be less than before. This can also be seen in Figure 5.20. The loss contribution for the transformer has decreased from 66 % to 35 %. However, the efficiency without the frequency dependence is assumed to be some kind of maximum efficiency while the efficiency with the frequency dependence is assumed to be some kind of minimum efficiency. This means that if the correct AC resistance can be calculated the efficiency would most likely be somewhere between the minimum and the maximum efficiency.

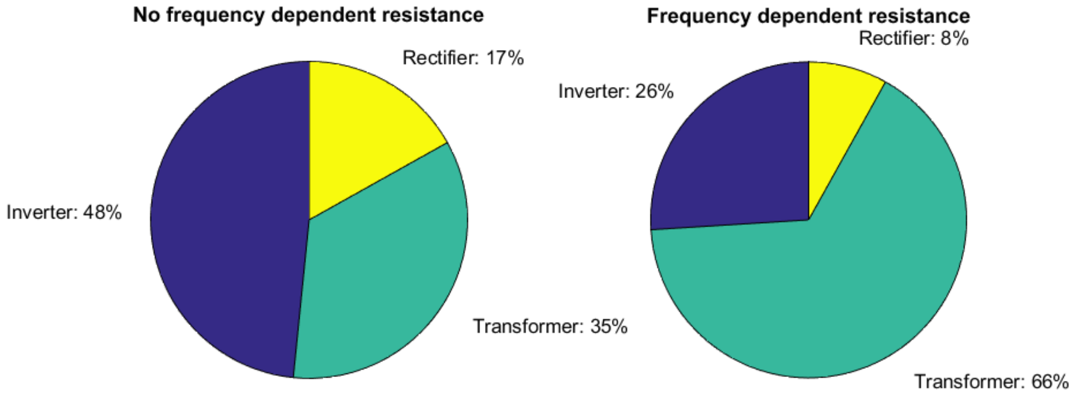

Figure 5.20: Loss distribution for the inductive cases with and without a frequency dependent resistance.

For inductive charging it is important to make sure that the charger can handle different distances and misalignment. This is due to that a EV will never park on the exact same spot every time. To be able to simulate these behaviour, k was swept from 0 to 1, the results of this can be seen in Figure 5.21. Due to that k is the connection between the primary and secondary coil $k = 0$ means that the distance between the coils is big and $k = 1$ means that the distance is absent. When k is close to zero, the connection between the coils will be almost absent, this means that the primary coil will act as a short circuit and this is why the input power is high while the output power is low compared to the input power. However, if k is increased, the input power drops while the output power increases due to that a connection between the two coils are established. This means that the efficiency will increase heavily due to the established connection and then stabilize. By increasing k even more both the input and the output power will continue to decrease. The efficiency remains the same until $k = 0.3$ where it starts to decrease slowly until $k = 0.8$ where it starts to decrease more. The decrease in efficiency can be caused due to that ZVS is not achieved anymore due to the small current.

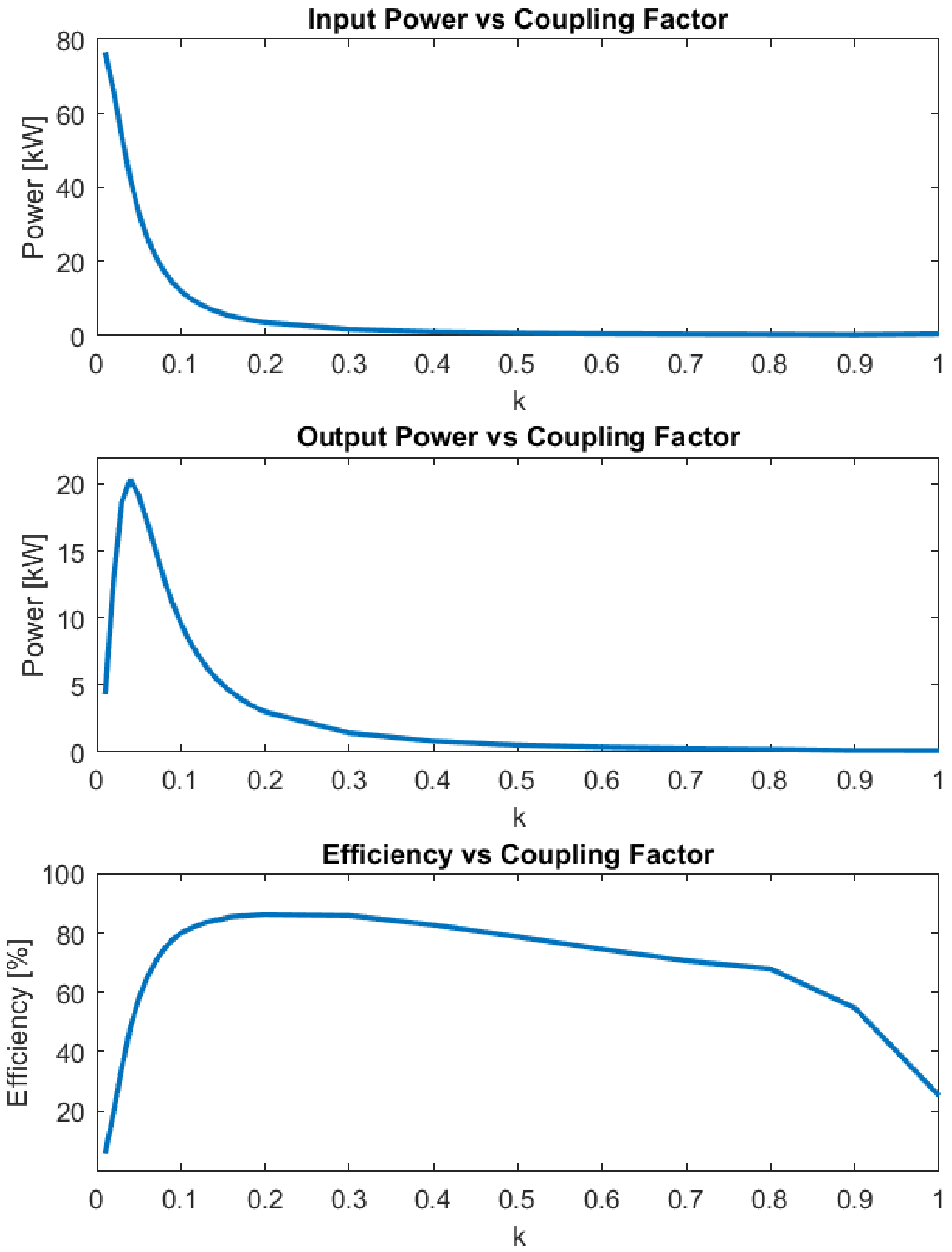

Figure 5.21: Output power for different coupling factors.

5.3 Cost analysis

A cost analysis of the system was made to see how much each separate system, would cost. The cost is measured in SEK, and is presented in Table 5.1. The leakage inductance for the conductive systems is included in the cost for the transformer due to that the transformer will either provide with the leakage inductance or some extra wire can be wired around a toroid to create the desired inductance. By looking at the table it can be seen that the inductive system costs 4695 SEK while the conductive systems costs between 3485 $-$ 3820 SEK. By adding the costs for the inductive and for the conductive systems the cost for two separate systems will be between 8180 $-$ 8515 SEK. To get the price for the combined system the costs for one boost converter, one inverter (4 MOSFETs) and one microcontroller can be removed. This means that 2225 SEK can be removed for the combined system which gives that the cost for the combined system in percent of the two separate system can be expressed as

$$\frac{4695\ SEK + 3615\ SEK - 2225\ SEK}{4695\ SEK + 3615\ SEK} = \frac{6085\ SEK}{8310\ SEK} = 73.2\% \tag{5.2}$$

$$\frac{4695\ SEK + 3820\ SEK - 2225\ SEK}{4695\ SEK + 3820\ SEK} = \frac{6290\ SEK}{8515\ SEK} = 73.9\% \tag{5.3}$$

$$\frac{4695\ SEK + 3485\ SEK - 2225\ SEK}{4695\ SEK + 3485\ SEK} = \frac{5955\ SEK}{8180\ SEK} = 72.8\%. \tag{5.4}$$

In the calculations, the costs are based on prices of single components which means that if the systems would have been mass produced the price for each system would decrease. However, how much money that can be saved in a mass production of the combined system in comparison to two systems is hard to predict.

Table 5.1: Costs of the inductive and conductive systems.

Part	Component	Ind - 450 V	Case 1	Case 2	Case 3
Boost	Diode ×5	5×230	5×230	5×230	5×230
	L	60	60	60	60
	MOSFET	80 [13]	80	80	80
	C	365	365	365	365
DC/DC step	MOSFET ×4	4×80	4×80	4×80	4×80
	Transformer	210	170	290	140
	Ferrite bars	450	N/A	N/A	N/A
	Diode ×4	4×230	4×230	4×230	4×230
	L_{out}	70	280	380	190
	C_{out}	5	20	5	10
	C_{comp}	815	N/A	N/A	N/A
Other	Microcontroller	250	250	250	250
	Total cost	4695	3615	3820	3485

6
Discussion

As was showed in the results, for inductive charging an efficiency of 85.98 % and 92.53 % was achieved for the simulations with and without a frequency dependence of the ESR for the transformer. The measurements of a similar system showed an efficiency of 93 %. The reasons for why the efficiency is so high for the measurements can depend on several reasons. One reason for the high efficiency is due to that the inverter is using SiC MOSFETs instead of Si MOSFETs. The SiC MOSFET provides with lower switching losses than a Si MOSFET and R_{on} for a SiC MOSFET will not increase as much as it will in a Si MOSFET when the temperature is increased[14].

The simulations showed an efficiency of 85.98 % with frequency dependence and a efficiency of 92.53 % without the frequency dependence. If the designed system would have been built the efficiency would probably be around $88 - 90$ % due to that the ESR will have a frequency dependence. However, it is complicated to estimate how much the frequency will affect the ESR with just calculations and it is also hard to measure an AC resistance with an instrument. One assumption can be that due to that a litz wire has a small frequency dependence, the correct ESR is closer to the calculated ESR without the frequency dependence than the ESR with the frequency dependence. This gives that the efficiency would be closer to 92.53 % than 85.98 %. However, the MOSFETs that was used in the simulations only provided with transient losses and conductive losses which means that heat losses and self heating is not included in the simulations. This means that if this model would have been built the efficiency for the system would probably be lower due to the excluded losses, but it is hard to tell how much these excluded losses will affect the efficiency. With this said a feasible efficiency for the inductive charging system would be between $88 - 90$ %.

For conductive charging an efficiency of around 98 % was achieved for Case 2 and 3 and for Case 1 an efficiency of 93 % was achieved. A conductive charger usually have a charging efficiency of around $94 - 95$ % [4]-[15] which gives that the simulations for the conductive cases provided with a efficiency that are a few percent higher than in the stated cases. One explanation for this can be that the MOSFETs, as mentioned before, only provides with transient losses and conductive losses. However, an efficiency of around $94 - 95$ % for the conductive charger would be desirable because then the chargers would be resembling to the chargers that are available today.

If the conductive models was supposed to be built it would be necessary to replace the chosen MOSFET with a MOSFET that can withstand higher a voltage level for Case 2. This is due to that the input voltage on the DC/DC step is 600 V in this case which only gives a safety margin of 17 %. For Case 1 and 3 the safety margin are around 55 % which is a good margin. MOSFETs with higher voltage ratings were tested but these MOSFETs caused problems during the simulations. The chosen MOSFET was the one with the highest voltage ratio that at the same time did not cause any problems during the simulation. The problem was that the time step for the simulation became too small in the simulation which interrupted the ongoing simulation. This can usually be fixed by adding ESR to the capacitors in the circuit or by lowering the tolerance and the quality of the simulations. However, these modifications did solve the problem for the MOSFETs with the higher voltage ratings. With this in mind, the best combined system will be based on the inductive case combined with Case 3. This is due to that it is desired to use the chosen MOSFET due to the low resistance, 37 $m\Omega$. Therefore Case 2 is not relevant due to the low safety margin. Case 1 and Case 3 have the same input voltage and therefore fulfils the safety margin but Case 3 was chosen due to that the efficiency was higher compared to Case 1. It is possible for future work, that Case 2 is redesigned with a input voltage of 450 V on the DC/DC step so the safety margin is fulfilled. The reason for why Case 2 is suggested to be redesigned is that 450 V as an output voltage for the charger is probably a better voltage level than 600 V due to that the voltage level for the battery is usually around 450 V and lower.

When it comes to the cost of the systems it was calculated that the inductive system would cost 4695 SEK and that the conductive systems would cost between 3485 $-$ 3820 SEK. The combined system would cost around 5955 $-$ 6290 SEK, however as was mentioned earlier, these costs are based on the price for individual components and if the system would be mass produced the cost would decrease. The cost could also be reduces by replace some of the components with cheaper components. For example, the chosen diode can withstand 1200 V which is twice as high as the voltage in Case 3, which has the highest voltage level of all cases. By choosing a diode with a voltage rating of 900 V for this case a safety margin of 50 % will still be achieved and the cost would be reduced a bit. The same argument can be made for case 1 and 2 were the voltage ratings are 100 V and 450 V, respectively.

It might be possible to reduce the costs of the charger by using components that are already installed in the EV. For example, to be able to run the motor in an EV, power electronics is needed and is therefore already installed in the car regardless if the EV is charged with an OBC or an off board charger. This means that it might be possible to reduce the costs of the components inside the car for the inductive part of the system by using some of the already installed components. For example, all EVs uses an inverter to convert the power from DC, from the battery, to AC for the motor. This inverter will not be used when the EV is charged which means that it could be used instead of the rectifier on the secondary side in the inductive part of the combined system. If this is possible, the passive rectifier will now be an active rectifier and most likely the losses will be reduced due to that MOSFETs usually have a smaller resistance compared to a diode.

The measurements showed that it is possible to achieve an efficiency of 93 % when charging wirelessly. However it is not as efficient as conductive charging yet and it also costs more. Inductive charging is on the other hand much easier to use due that the only thing the driver needs to do is to park over the primary coil. This also means that the user never needs to touch a cable in a humid environment which means that the risk of getting a electric shock from the cable is absent. This makes the inductive charging system much safer than the conductive charging system. With this said, inductive charging is a strong competitor to conductive charging when it comes to charging an EV for 3.3 kW. Therefore, an interesting test scenario would be to test a combined system that could handle inductive charging and fast charging. For this test scenario inductive charging would have been used for normal loading as in this project and conductive charging would have been used for fast charging. This system would in theory provide with a convenient way of charging a EV at home or at work with inductive charging and still provide with the possibility to fast charge an EV.

6.1 Sustainable Development and Ethical Aspects

This section will first discuss the questions that was asked in the introduction about sustainable development and second the ethical aspects will be discussed. So how is a better charger for an EV going to make the world more sustainable? As mentioned in the introduction, most of the vehicles on the streets are equipped with a combustion engine and these vehicles are producing a huge amount of green house gases. By replacing the combustion vehicle with EVs it is possible to reduce the amount of green house gases, provided that the amount of green house gases from the combustion vehicles is higher than the amount of green house gases from the production of the electricity that the EV is charged with. By making it easier and more convenient for the driver to charge the EV with inductive charging the amount of EVs can hopefully get a push on the market and the EV can hopefully compensate for the lower mileage with its extremely simple way of charging. However, this assumes that the EVs are replacing the combustion vehicles and not just added on to the amount of already existing vehicles. However, it is not likely that people will buy an EV and at the same keep the old combustion vehicle due to the costs of it. Therefore, a qualified assumption would be that by introducing inductive charging for EVs the chances of replacing combustion vehicles with EVs are increased which in the end will reduce the amount of green house gases in the world.

The economical aspects is directly connected to the cost of the charger and it was presented in the previous chapter. However, the cost is just representing one system and if a mass production will take place the cost will reduce heavily. The cost is an important factor due to that people might just see the cost of installing a EV charger at home as an extra cost for buying a EV. For example, when buying a combustion car you do not need to buy a gas station, the only thing that costs money is the gas. For an EV this is not the case, when buying an EV it is also necessary to buy a charging station and install it in the garage or in the carport. However, it is important to state that the costs after the EV is bought and installed is lower than the gas price, for most countries. This means that over time more money will be spent on gasoline than on the EV charger plus the electricity. It is also important that governments are funding EV chargers not just in the big cities but also in smaller towns and along the highways. Otherwise it is just possible to drive shorter distances and the EV will not be an alternative for the people who commute by car to work everyday. One small step could be to install charging stations at work so it is possible to charge the EV during work hours.

As mentioned there are three aspects to be taken into consideration when discussing if a better charger for an EV going to make the world more sustainable? And even if the ecological aspects is the most relevant, followed up by the economical, the social aspects needs to be discussed in this project as well. One thing that is needed to be able to replace the combustion cars with EVs is as mentioned before that governments are willing to spend money. If the cities are not offering charging station people might need to drive ridiculous distances just to charge the EV, which in the end is not sustainable at all.

When it comes to the ethical part of this project the most important ethical statement is defined as "Show correct results from the simulations and the conclusions that are made should be backed up with correct data". The data for this project was presented in the previous chapter and as could be seen the results showed that power could be transferred both wireless and through a cable with a high efficiency. Both the conductive and the inductive chargers was tested with different duty cycles and was tested for different load levels. The inductive charger was also tested for different distances. All these different simulations can be added together and provide an overall impression on what these systems are capable of. The characteristics for the conductive systems are similar to each other which strengthens the credibility of the provided data. Also, the characteristics from the simulations of the inductive systems are similar to the measurements which also strengthens the credibility. Last, the efficiency for the all systems was compared to other systems from other projects which also proves that the data from this project is reliable. The conclusion can be seen in the following chapter and all conclusions are based on the data provided from the previous chapter. This gives that the conclusions that were made are backed up with correct and accurate data. The last ethical topic is about safety. The magnetic field can cause damage on humans and animals if exposed to the magnetic field. The damages that it can cause is dependent on how strong the magnetic fields are and how often one is exposed to it. Therefore it is extremely important to avoid the magnetic fields when inductive charging is used. As mentioned earlier, ferrite bars can concentrate the magnetic fields which means that not only the efficiency will increase but also the safety of the system will increase. It is also important that animals are protected from these magnetic fields when an EV is charged. For example, a cat could crawl under the EV during winter times to protect itself from the cold weather. The inductive system which will generate heat might than be a perfect place for the cat to warm up itself. These situations has to be avoided due to that the cat can be severely damaged by the magnetic fields.

Therefore a screen or a similar object might be necessary the the EV is charged on a car port. If the EV is charged in a garage it is enough to just make sure that the cat is not inside the garage when the EV is charged inductively.

7
Conclusion

It has been shown that it is possible to design a system that can handle both conductive and inductive charging in an efficient way. This was done by combining an off board charger with an inductive charger. The combined system consists of a boost converter and one DC/DC step. The DC/DC step is divided into one inductive part and one conductive part and the DC/DC step consists of one inverter, two transformers, two capacitor banks and two rectifiers. This gives that the inductive and the conductive part shares the same inverter.

Two boost converters were designed, one with an output voltage of 450 V and one with an output voltage of 600 V. The efficiency for the two boost converters was over 99 % and could supply the DC/DC step with the desired voltage with a voltage ripple of 1 V. However, if the boost converter would have been built, the efficiency would decrease due to that the simulations did not take all kind of losses in concern.

The efficiency for the inductive DC/DC step where the ESR had a frequency dependence was 85.98 % for an input voltage of 450 V and a duty cycle of 0.7. By increasing the duty cycle to 0.9 the efficiency can be increased to 88 %. By excluding the frequency dependence of the ESR an efficiency of 92.53 % was achieved for $D = 0.7$. Measurements were performed on a prebuilt inductive charger with SiC MOSFETs and the measurements showed that an efficiency of 93 % could be achieved. The simulations for the conductive case showed an efficiency of 98.42 % 98.06 % for Case 2 and 3, respectively, while Case 1 had an efficiency of almost 93 %.

The cost for the inductive systems was calculated to be 4695 SEK and the cost for the three conductive cases was calculated to be 3615 $SEK4$, 3820 SEK and 3485 SEK. By combining the inductive and the conductive systems the total cost for the combined systems was calculated to be 6085 SEK, 6290 SEK and 5955 SEK, which means that the cost for a combined system would be $72.8 - 73.9$ % of the total cost of one inductive and one conductive system.

It was decided that the combined system should be based on the inductive system and Case 3. This was due to that Case 3 was the only case that provided with a high efficiency and an acceptable safety margin for the chosen MOSFET. The cost for this system was calculated to 5955 SEK.

Bibliography

[1] Statistics Sweden, "Registered passenger cars in use, 1923–2016," 16 February 2017. [Online]. Available: http://www.scb.se/en/finding-statistics/statistics-by-subject-area/transport-and-communications/road-traffic/registered-vehicles/. [Accessed: 9 June 2017].

[2] Statistics Sweden, "Registered vehicles January 2006–May 2017" 2 June 2017. [Online]. Available: http://www.scb.se/tk1001-en. [Accessed: 9 June 2017].

[3] Swedish Radiation Safety Authority, "Magnetic fields and wireless technology - Magnetic fields," 13 December 2012. [Online]. Available: http://www.stralsakerhetsmyndigheten.se/In-English/About-the-Swedish-Radiation-Safety-Authority1/Magnetic-fields-and-wireless-technology/Magnetic-fields/. [Accessed: 25 January 2017].

[4] S. Haghbin and T. Thiringer, A 3.3 kW Onboard Battery Charger for PHEVs. Göteborg: Chalmers University of Technology, 2015.

[5] D. K. Cheng, Field and Wave Electromagnetics. Harlow, Essex, England: Pearson, 2014.

[6] P.Höjevik, "Informationsbehov rörande elsäkerhet kring laddinfrastrukturen för elbilar," Elsäkerhetsverket, 2014. [Online]. Available: http://www.elsakerhetsverket.se/globalassets/publikationer/rapporter/elsak_informationsbehov_laddningsinfrastruktur_2014.pdf. [Accessed: 15 September 2017].

[7] European Commission, "EU launches clean fuel strategy," 24 January 2013 [Online]. Available: http://europa.eu/rapid/press-release_IP-13-40_en.htm. [Accessed: 15 September 2017].

[8] European Commission, "European Parliament vote "milestone" in the roll out of clean fuels for transport," 14 April 2014 [Online]. Available: https://ec.europa.eu/transport/themes/urban/news/clean-fuels-transport_en. [Accessed: 15 September 2017].

[9] Vattenfall, "Wireless charging of future electric cars," 6 May 2015 [Online]. Available: http://news.vattenfall.com/en/article/wireless-charging-future-electric-cars. [Accessed: 17 September 2017].

[10] K. Woronowicz et al. Boucherot bridge based zero reactive power inductive power transfer topologies with a single phase transformer. 2014, . DOI: 10.1109/IEVC.2014.7056229.

[11] Raggl et al, "Comprehensive Design and Optimization of a High-Power-Density Single-Phase Boost PFC," IEEE Transactions on Industrial Electronics, vol. 56, pp. 2574-2587, 2009.

[12] M. Chinthavali et al. Isolated wired and wireless battery charger with integrated boost converter for PEV applications. 2015, . DOI: 10.1109/ECCE.2015.7309745.

[13] AVNET, Available: https://www.avnet.com. [Accessed: 9 June 2017].

[14] J. Biela et al. SiC vs. si-evaluation of potentials for performance improvement of power electronics converter systems by SiC power semiconductors. 2010, . DOI: 10.4028/www.scientific.net/MSF.645-648.1101.

[15] D. Gautam et al. An automotive on-board 3.3 kW battery charger for PHEV application. 2011, . DOI: 10.1109/VPPC.2011.6043192.